

Molecular Absorption Test at 35 GHz

H.J. Liebe



U.S. DEPARTMENT OF COMMERCE
Malcolm Baldrige, Secretary

Bernard J. Wunder, Jr., Assistant Secretary
for Communications and Information

February 1982

PREFACE

The author gratefully acknowledges the following persons for their contributions to this report:

- Mr. Vince Wolfe and Ms. M. Kemp
University of Colorado
Boulder, CO 80306,
who provided technical assistance and performed some (e.g., N_2O
and NO_2 by Ms. Kemp) of the measurements;
- Mr. Dale Divis
Lockheed Research and Development
Huntsville, AL 35807,
who formulated the problem;
- Prof. Frank C. DeLucia
Physics Dept. Duke University
Durham, NC 27706,
who furnished unpublished computer printouts of line center
frequencies for HNO_3 and HNO_2 ;
- Dr. C. J. Howard
NOAA-ERL-Aeronomy Laboratory
Boulder, CO 80303,
who provided samples of the test gases and invaluable counsel
on their chemical properties.

This work was sponsored by the Defense Nuclear
Agency under Task Code Q 78QAxHD, Work Unit 00001,
and Order No. 81-834, 1ACRO.

TABLE OF CONTENTS

	Page
LIST OF FIGURES.	vi
LIST OF TABLES	vii
EXECUTIVE SUMMARY.	viii
ABSTRACT	1
1. INTRODUCTION.	1
2. THEORY OF GASEOUS MOLECULAR ABSORPTION.	2
2.1 Pressure-Broadened Line Absorption	7
2.2 Pressure-Broadened Band Absorption	8
2.3 Debye Absorption	8
3. SPECTROMETER PERFORMANCE AT 35 GHz.	10
3.1 Test Requirements.	10
3.2 Detection Sensitivity and Stability.	11
3.3 Intensity Calibration.	13
4. GAS HANDLING.	13
4.1 Precautions.	15
4.2 Measurement Strategy	18
5. RESULTS AND DISCUSSION	18
5.1 Water Vapor (H_2O).	19
5.2 Hydrogen Peroxide (H_2O_2)	21
5.3 Nitric Acid (HNO_3)	21
5.4 Nitrogen Oxides (NO_2, N_2O).	21
6. MODELING	27
6.1 Sea Level Behavior of Normal Moist Air	27
6.2 One Atmosphere of Hot Air.	27
7. CONCLUSIONS	29
8. REFERENCES	30
APPENDIX: PRESSURE-SCANNING MM-WAVE SPECTROMETER.	33

LIST OF FIGURES

	Page
Figure 1. Normalized Lorentzian frequency and pressure profiles of an isolated line for absorption and dispersion.	6
Figure 2. Pressure profiles of the O_2 microwave spectrum at 300 K for two cases: (a) in the vicinity of 9+ line, (b) the band shape continuum between 51 and 61 GHz.	6
Figure 3. Time series of minimum detectable attenuation and refractivity .	12
Figure 4. Simulated absorption for absolute attenuation calibration. . . .	12
Figure 5. Schematic of gas handling system	14
Figure 6. Saturation pressure of nitric acid vapor	16
Figure 7. Decay of nitrous acid concentration inside 12 liter Pyrex mixing chamber	16
Figure 8. Water vapor attenuation and refractivity at 35 GHz as a function of the vapor pressure at room temperature	20
Figure 9. Gaseous hydrogen peroxide attenuation and refractivity at 35 GHz as a function of pressure at room temperature.	22
Figure 10. Gaseous nitric acid attenuation and refractivity at 35 GHz as a function of pressure at room temperature	23
Figure 11. Nitrous oxide attenuation and relative refractivity at 35 GHz as a function of pressure and temperature.	24
Figure 12. Determination of the molecular dipole moment of nitrous oxide. .	24
Figure 13. Attenuation predictions for moist air at sea level over the frequency range 10-50 GHz at four temperatures between -20 and 40°C	26
Figure 14. Attenuation predictions for hot air at sea level pressure and constant humidity over the frequency range 10-50 GHz and temperatures between 200 and 500 K	28
<hr/>	
Figure A1. Schematic of the pressure-scanning spectrometer.	34
Figure A2. Construction details of the Fabry-Pérot resonator for operation in the 26.5-40 GHz band.	36
Figure A3. Circuit diagram of phase marker and peak level detector.	38
Figure A4. Block diagram of time interval averaging for refraction.	38

LIST OF TABLES

	Page
Table 1. Absorption Line Properties in the Vicinity of 35 GHz.	4
Table 2. Test Conditions for 35 GHz Molecular Absorption Study	10
Table 3. Maximum Vapor Pressure of Liquid H_2O_2 - H_2O Mixtures.	17
Table 4. Attenuation by Nitrogen with Traces of HNO_3	25

EXECUTIVE SUMMARY

Systems operating at 35 GHz might have to function in environments polluted by (> 100 ppm/v) the molecules H_2O_2 (hydrogen peroxide), HNO_3 (nitric acid), HNO_2 (nitrous acid), NO_2 (nitrogen dioxide), and N_2O (nitrous oxide). The question was posed as to whether any of these molecules will cause substantial absorption (> 0.25 dB/km) near 35 GHz, in addition to that caused by H_2O and O_2 . A laboratory experiment was prepared to measure, at room temperatures, absolute attenuation-versus-pressure rates of the identified molecular species. The difficulties with the experiment lie in the corrosive, adsorptive, and hazardous nature of the test vapors and in achieving (a) a high detection sensitivity (< 0.1 dB/km) with absolute calibration and (b) a verified concentration inside the test cell.

A brief discussion of the absorption mechanisms, such as spectral lines, bands, and pressure-induced effects, is given. A pressure-scanning resonance spectrometer was operated and its performance was optimized and assessed around 35 GHz. Measurements of attenuation and refraction were performed on fairly pure vapors at low pressures (< 1 kPa) and on mixtures at atmospheric pressures (> 50 kPa) using N_2 as the inert, loss-free host gas. The molecules H_2O , H_2O_2 , N_2O , NO_2 , and HNO_3 produced within the uncertainties of the experiment insignificant attenuation (< 0.2 dB/km) up to concentrations of 500 ppm/vol in 1 atm of air. The chemistry of generating the highly unstable nitrous acid (HNO_2) was not mastered, and these measurements proved to be unsuccessful.

The report concludes with model calculations of attenuation for sea level air which were performed over the frequency range 20 to 50 GHz: (1) for the temperature range -20° to 40°C and relative humidities $\text{RH} = 0, 10, 50, 100$ percent, and (2) for 200 to 500 K.

MOLECULAR ABSORPTION TEST AT 35 GHz

Hans J. Liebe^{*}

This report describes a laboratory experiment which was conducted to find out if the absolute attenuation of a 35 GHz signal by the molecular species H_2O_2 (hydrogen peroxide), HNO_3 (nitric acid), NO_2 (nitrogen dioxide), and N_2O (nitrous oxide) exceeds a threshold value of 0.2 dB/km for concentrations reaching 500 ppm/vol in 1 atm of air. A resonance spectrometer was operated with a detection sensitivity of 0.1 dB/km to obtain pressure scans of attenuation and refraction for the pure gases at low pressures (< 1 kPa) and for binary mixtures at atmospheric pressures (> 50 kPa) using nitrogen as the inert, loss-free host gas. Model calculations of attenuation over the frequency range 10 to 50 GHz were performed for natural moist air and hot air (< 500 K) under sea level conditions. The measurements of the identified trace gas species produced little (< 0.2 dB/km) additional attenuation.

Key words: atmospheric 35 GHz attenuation; laboratory measurements; model calculations; trace gas absorption

1. INTRODUCTION

Systems are planned for operation at 35 GHz through a polluted atmosphere. There has been concern whether increased concentration of molecules of certain chemical species would lead to additional loss. In particular, the polar molecules H_2O_2 , HNO_3 , HNO_2 , NO_2 , and N_2O in enhanced concentrations (> 100 ppm/vol) are likely candidates for causing absorption (> 0.25 dB/km) around 35 GHz, in addition to those present in natural air (H_2O and O_2). The origin of such molecular absorption can lie in the following physical mechanisms:

- o strong local spectral lines
- o low frequency wing response of an intense rotational band
- o nonresonant excess absorption due to pressure-induced dipole moments of temporary molecular pairs (Meier, 1979).

The intensity of the absorption is determined primarily by the magnitude of the molecular dipole moment, the number of absorbing molecules, the total number of molecules, and the frequency.

In normal moist air, the frequency of 35 GHz is flanked on one side by the 22 GHz H_2O absorption line and on the other by the 60 GHz O_2 band. The confidence in predicting molecular absorption due to H_2O and O_2 is quite high (less than

^{*}

The author is with the U.S. Department of Commerce, National Telecommunications and Information Administration, Institute for Telecommunication Sciences, Boulder, Colorado 80303.

3% uncertainty) assuming that pressure, p ; temperature, T ; and relative humidity, RH , are known. A detailed computer program for the full altitude range $h = 0$ to 100 km has been developed, which is valid up to 1000 GHz (Liebe, 1981).

Both computational and experimental methods can be used to determine the absorption coefficients for trace molecules. However, it was felt that a properly performed experiment could determine absorption rates with the least amount of uncertainty. Accordingly, the following sections provide details of the effort required for a controlled molecular absorption experiment using the pressure-scanning resonance spectrometer described in the APPENDIX.

Microwave rotational spectroscopy is a sensitive experimental research method for investigating gaseous pollutants and atmospheric constituents in the environment. The technique measures absorption, α (dB/km) and refractivity, N' (ppm). The limitation to the performance of such an instrument is the threshold detection limit, which must be better than 0.1 dB/km and 0.05 ppm. Further difficulties with the experiment lie in the corrosive, absorptive, and hazardous nature of the test vapors and in achieving a verified concentration inside the test cell.

2. THEORY OF GASEOUS MICROWAVE ABSORPTION

A radio wave propagating at 35 GHz, close to ground level and through a cloudless atmosphere, suffers loss and delay effects due to molecular absorption in moist air (caused mostly by H_2O and O_2). Amplitude and phase response of a planar wave traveling the distance L and starting with the field strength E_0 is described by

$$E = E_0 \exp [j0.0210\nu (10^6 + N)L] \quad (1)$$

where the frequency ν is in gigahertz (GHz), the refractivity N is in parts per million (ppm), and the path length L is in kilometers (km). A convenient macroscopic measure of the interaction between radiation and the absorbing species in moist air is the complex refractivity N (ppm), expressed in terms of measurable quantities. For air, N consists of three components

$$N = N_0 + D(\nu) + j N''(\nu) \quad (\text{ppm}) \quad (2)$$

namely, the frequency independent refractivity N_0 plus various spectra of refractive dispersion $D(\nu)$ and extinction $N''(\nu)$. Usually, the imaginary part of (2) is expressed as the power attenuation rate

$$\alpha = 0.182 \nu N'' \text{ (dB/km)} \quad (3)$$

and the real part determines the excess propagation delay time

$$t = 3.34 (N_0 + D) \text{ (ps/km)}. \quad (4)$$

Frequency-Independent Refractivity of moist air is given by

$$N_0 = [2.589 P + (41.6 \theta + 2.39) e] \theta \text{ (ppm)}. \quad (5)$$

The symbols are defined as follows:

$$\begin{aligned} P &= \text{dry air pressure} && \text{(kPa)}, \\ e &= \text{partial water vapor pressure} && \text{(kPa)}, \\ \theta &= 300/T = \text{relative inverse temperature} && \text{(T in K)}. \end{aligned}$$

This study is directed at an experimental evaluation of attenuation α for simulated low-altitude atmospheric conditions that are polluted by the trace molecules H_2O_2 , HNO_3 , HNO_2 , and N_2O . Table 1 lists the known properties of lines reported in the vicinity of 35 GHz. These local lines and their complete spectra are assumed to be a main cause of attenuation.

Absorption and Dispersion Spectra are formulated from line and continuum contributions; that is

$$N''(\nu) = \sum_i (S F'')_i + N''_C \text{ (ppm)} \quad (6)$$

and

$$D(\nu) = \sum_i (S F')_i \text{ (ppm)} \quad (7)$$

where $i = 1, 2, 3 \dots$ is a label for each line and

$$\begin{aligned} S &= \text{line strength} && \text{(kHz)}, \\ F''(\nu) &= \text{absorption line shape} && \text{(GHz)}^{-1}, \\ F'(\nu) &= \text{dispersion line shape} && \text{(GHz)}^{-1}, \\ N''_C(\nu) &= \text{continuum absorption} && \text{(ppm)}. \end{aligned}$$

Attenuation in the vicinity of an isolated, pressure-broadened ($p > 3 \text{ Pa}$) line is described by a Lorentzian line shape, yielding (see Figure 1)

Table 1. Absorption Line Properties in the Vicinity of 35 GHz

Molecule	Center Frequency ν_0	Quantum No. ID		Max J Value	Peak Line Attenuation α_0 (ν_0 , 300K)	Reference
		J	J'			
	GHz	Lower	Upper		dB/km	
H ₂ O ($\mu=1.85$)	22.23580	5 2 3	6 1 6	≤ 15	3.15	b
	27.6396	8 5 1	9 6 1(ν_4)			c
H ₂ O ₂ ($\mu=1.58$)	34.56	?				d
	35.916	High J		≤ 12		e
	37.518298	1 0 1	2 1 1(ν_2)		+	c
	39.19463	20 3 17	21 2 19			k
	39.49460	11 11 0	12 0 12(ν_3)			c,d
HNO ₃ ($\mu=2.16$)	30.8816	1 1 1	2 1 2		+	f
	31.79280	1 0 1	2 1 2		+	f,g
	33.09084	6 4 3	6 5 2			a
	33.31293	5 1 5	4 4 0			a
	33.63015	6 3 3	6 5 2	≤ 12		a
	34.66272	6 4 2	6 6 1			a
	35.10991	4 3 1	5 2 4		+	a
HNO ₂ ($\mu=3.2$)	32.73959	9 2 7	10 1 10			h
	33.30219	1 1 1	2 0 2		+	a
	36.50198	11 2 9	12 1 12	≤ 12		a
	37.5176	1 0 1	2 1 2		+	a

(Continued next page)

Table 1. Absorption Line Properties in the Vicinity of 35 GHz (Cont'd)

Molecule	Center Frequency ν_0	Quantum No. ID		Max J Value	Peak Line Attenuation α_0 (ν_0 , 300K)	Reference
		J	J'			
	GHz	Lower	Upper		dB/km	
N ₂ O ($\mu=0.161$)	25.1233	0	1	≤ 2	1.7	i
	50.2464	1	2		13.5	i
NO ₂ ($\mu=0.316$)	26.569	23 2 22	24 1 23	≤ 25	0.83	i
	39.247	22 1 21	21 2 20		1.8	i
O ₂ (μ_{magnetic})	38 lines between 50 and 69 GHz	K = 1 ⁺ to 37 ⁺		≤ 38	65(60 GHz)	b (Figure 2)
	61.15057	K = 9 ⁺			9.9	b

μ in debye is the molecular dipole moment,

+ expected strong absorption lines.

References:

- a) Bowman et al., 1981a, and DeLucia, private communication, 1980
- b) Liebe, 1981
- c) Helminger et al., 1981
- d) Hunt et al., 1965
- e) FMC, 1969
- f) Cazzoli and DeLucia, 1979
- g) Millen and Morton, 1960
- h) Varma and Curi, 1976
- i) Kolbe et al., 1977
- k) Bowman and DeLucia, 1981b.

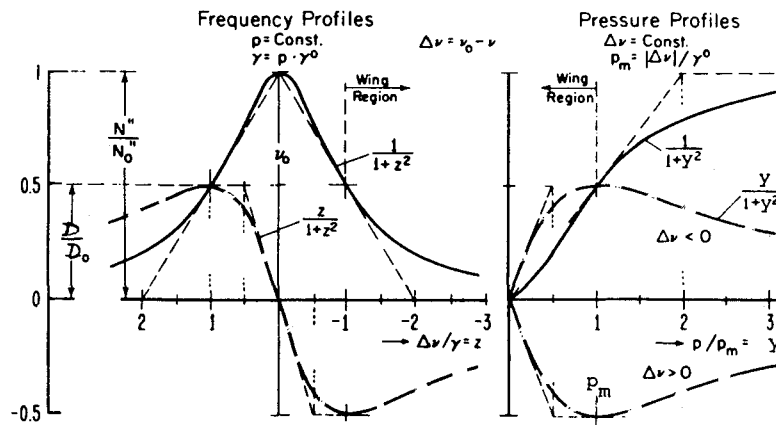


Figure 1. Normalized ($S^0 = \gamma^0$) Lorentzian frequency (z) and pressure (y) profiles of an isolated line for absorption N'' and dispersion $D = N' - N_0$.

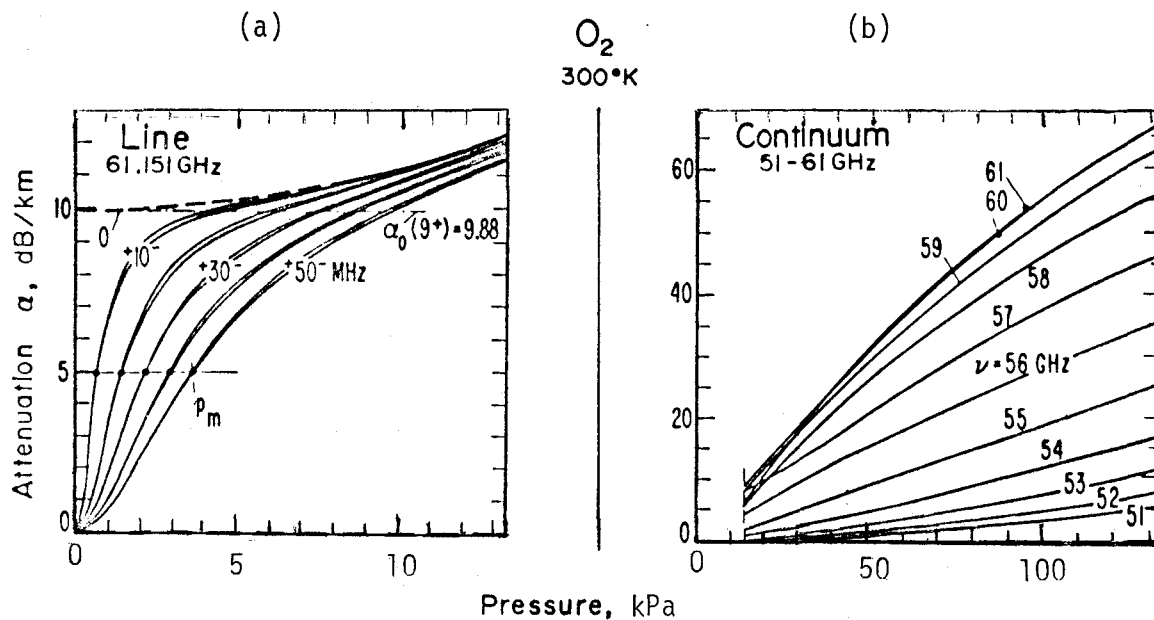


Figure 2. Pressure profiles of the O_2 -MS at 300K for two cases: (a) in the vicinity ($\nu_0 \pm 50$ MHz) of the 9^+ line, (b) the band shape continuum between 51 and 61 GHz.

$$\alpha = \alpha_0 / (1+z^2) \quad (8)$$

where $\alpha_0 = 0.182 \nu_0 S / \gamma$ is the peak attenuation at ν_0 , $z = (\nu_0 - \nu) / \gamma$ is the normalized frequency, and γ is the linewidth.

From Table 1 it is apparent that quantitative data on α_0 for the species H_2O_2 , HNO_3 , and HNO_2 are missing. These can, in principle, be calculated from molecular data (Poynter and Pickett, 1980); however, for this study it was decided that measurements of α around 35 GHz would suffice.

Attenuation α [(3), (6), (8)] and refractivity $N' = N_0 + D$ [(4), (5), (7)] are measured at a fixed frequency and temperature with the resonance spectrometer described in the APPENDIX. A detection sensitivity of 0.1 dB/km is achieved with a high Q value design employing a Fabry-Pérot resonator (Figure A2), which assures a long effective path length, L_R (Eq. A5). When an absorbing gas is introduced into the evacuated resonator cell, both the Q value (Eq. A2) and the resonance frequency ν_R (Eq. A6) are lowered with increasing gas pressure.

In the following sections, three types of expected output from the pressure-scanning spectrometer are briefly analyzed assuming the idealized cases of an isolated line, a band shape of a line spectrum, and nonresonant absorption due to pressure-induced effects. These model-cases provide the basis for discussing experimental results.

2.1 Pressure-Broadened Line Absorption

Microwave lines of polar gas molecules normally appear at low pressure (< 1 kPa) as isolated features. For pressure broadening, both frequency and pressure profiles are expected to be Lorentzian, as illustrated in Figure 1. Lorentzian absorption and refraction pressure profile are described by

$$N_L'' = (S^0 / \gamma^0) y^2 / (1 + y^2) \quad (\text{ppm}), \quad (9)$$

$$N_L' = N_0 \pm D = N_0^p \pm (S^0 / \gamma^0) y / (1 + y^2) \quad (\text{ppm}). \quad (10)$$

The pressure is normalized by $y = p / p_m$, whereby the reference pressure is approximately [i.e., neglecting refractive tuning $\nu_R(1 - N_p^0)$]

$$p_m \approx (\nu_0 - \nu_R) / \gamma^0 \quad (\text{kPa}). \quad (11)$$

Center frequency ν_0 and the pressure-proportional parameters of refraction N^0 , strength S^0 (Hz/kPa), and width γ^0 (MHz/kPa) describe the profiles at constant temperature T . The spectrometer is tuned to ν_R and takes pressure scans of $N''(p)$ and $N'(p)$ simultaneously. From a family of pressure profiles recorded with a pure, resonant gas at different settings of ν_R it is possible to deduce the spectroscopic parameters N^0 , ν_0 , γ^0 , and S^0 (Liebe, 1975).

2.2 Pressure-Broadened Band Absorption

The oxygen microwave spectrum shall serve as a representative example of a band. Many (> 40) lines are clustered around 60 GHz, with one exception (119 GHz), and they overlap appreciably at sea-level pressures. All line parameters (ν_0 , S^0 , γ^0) are well known. A correct description of the band shape requires use of overlapping line theory (Liebe, 1981). Figure 2 depicts the behavior of various O_2 pressure profiles. The calculation, based on the sum of 44 Lorentzian lines

$$\alpha = 0.182 \nu \sum_{i=1}^{44} N_L''(p)_i \quad (\text{dB/km}), \quad (12)$$

is valid to first order for $p = 1$ to 100 kPa. Line (a) and continuum (b) profiles can be distinguished. In the vicinity of a line it is possible to separate line (Eq. 9) and band spectra by formulating

$$\alpha = 0.182 \nu (N_L'' + K'' p^2). \quad (13)$$

The value of K'' is a constant for a particular line. Band pressure profiles above 20 kPa are more difficult to interpret quantitatively. Assuming that for all i lines the parameters ν_0 , S^0 , and γ^0 are known, then experimental $\alpha(p)$ profiles can be compared with the simple prediction of equation (12). Any deviations are attributable to interfering overlap effects.

2.3 Debye Absorption

Nonresonant microwave absorption can occur when additional dipole moments are generated by short-lived pairs of colliding polar molecules. The limited lifetime of these pairs leads to a Debye-shaped continuum absorption (Meier, 1979)

$$N_C'' = (2\pi/3kT) M_1 \mu_1^2 \nu_T / [1 + (\nu_T)^2] \quad (\text{ppm}) \quad (14)$$

where $M_1 \approx (2MM')^{1/2}$ (cm^{-3}) is the approximate concentration of molecular pairs,

$\tau \approx 2\pi r(m_1/2kT)^{1/2}$ (s) is the relaxation time,
 μ_1 is the effective dipole moment which can be estimated from the known
dipole moments and polarizabilities of the interacting molecules,
 m_1 is the reduced mass of the molecular pair, and
 r is the intermolecular distance.

Low values of τ , large dipole moments, and a close approach favor the generation of collision-induced Debye absorption.

Meier (1979) measured, at 94 GHz and 297°K the value $\alpha_c \approx 0.5$ dB/km for the system $\text{SO}_2(30 \text{ Pa}) + \text{H}_2\text{O}(3 \text{ kPa})$. The possibility exists that, in moist air, $\text{H}_2\text{O} - \text{H}_2\text{O}$ and $\text{H}_2\text{O} + \text{X}$ ($\text{X} =$ other dipole molecule, see Table 1) pairs are responsible for non-resonant microwave absorption.

In Summary--theory provides the following guidance for directing the experimental effort:

- (a) A pressure scan $\alpha(p)$ with a pure, absorbing gas reaches at low pressures (<1 kPa) the plateau α_0 (Eqs. 8,9) when linecenter (ν_0) and test (ν_R) frequencies are close on a megahertz scale.
- (b) The same scan displays a functional form $\alpha(p) \propto p^2 < \alpha_0/2$ (Eqs. 9,13) when the frequency separation is larger than the width $\gamma = \gamma^0 p$, where typically $\gamma^0 = 50$ to 200 MHz/kPa.
- (c) In case the absorbing gas (p) is diluted by a loss-free host gas ($P \gg p$), a much smaller line maximum (Eq. 8)

$$\alpha_0^f \approx 0.182 \nu_0 (S^0/\gamma_f^0)(p/P) \quad (\text{dB/km}) \quad (15)$$

is expected since $\gamma_f \approx \gamma_f^0 p$, whereby P is the total pressure. Typically, $\gamma_f = (0.2 \text{ to } 0.5) \gamma^0$. For this study, the following conditions apply:

$$p/P \leq 10^{-4} \quad \text{and} \quad \alpha_{\min} \geq 0.2 \text{ dB/km at } \nu \approx 35 \text{ GHz,}$$

which require line absorption values α_0 on the order of 1000 dB/km and $\nu_R = \nu_0$. This is an unreasonable expectation at the "low" frequency of 35 GHz since α_0 is proportional to ν_0^2 . Line strengths of this magnitude are known above 300 GHz.

- (d) In the presence of high concentrations of polar molecules, the nonresonant Debye absorption (14) might play a role.

3. SPECTROMETER PERFORMANCE AT 35 GHz

Performance criteria of a spectrometer relate to such key factors as sensitivity, stability, systematic errors, and intensity calibration. The instrument was originally developed for quantitative studies of the 60 GHz O_2 band (Liebe, 1975). It was substantially modified and improved to meet or to exceed the test requirements at 35 GHz. A complete description of the resonance spectrometer, details of the alterations, and operational procedures are presented in the APPENDIX. At this point, we are mainly concerned with the minimum detectable attenuation α_{\min} , its stability, and its absolute calibration in units of dB/km.

3.1 Test Requirements

The general test requirements for the 35 GHz molecular absorption test are summarized in Table 2 (specified by sponsor). The pressure-scanning resonance spectrometer (see APPENDIX), which is used to perform the measurements, is the most sensitive instrument available for quantitative studies requiring the full pressure range between 0 and 1 atmosphere (1 atm \equiv 760 torr \equiv 1013 mb \equiv 101.3 kPa). At one frequency (ν_R), an effective interaction path length of several hundred meters can be realized.

Table 2. Test Conditions for 35 GHz Molecular Absorption Study

VARIABLE		MAGNITUDE	COMMENTS
Frequency Range		35 \pm 2% GHz	
Accuracy		0.01 GHz or less	\pm 5 kHz during test
Minimum Absorption Rate		0.25 dB/km	Absorption rates less than .25 dB/km are insignificant
Accuracy		\pm 0.05 dB/km	
Species	X	$H_2O, H_2O_2, HNO_3, (HNO_2), N_2O,$ NO_2 (see Table 1)	
Absorber Concentration	M	10^{16} to 10^{12} cm^{-3}	$M = 2.44 \times 10^{14}$ p(Pa) cm^{-3} (ideal gas law at 25°C)
Temperature	T	24 to 26, (10 to 70 for N_2O), \pm 0.1°C	
Total Pressure	P	10 to 100 kPa	Host Gas: N_2
Absorber Pressure	p	40 to 4×10^{-3} Pa	1 Pa \equiv 10^{-2} mb

3.2 Detection Sensitivity and Stability

The peak detector of the pressure-scanning spectrometer (see APPENDIX) records an absorption pressure profile (Eq. A4)

$$a_1(p) = a_0 / [(\alpha(p)L_R/4.34) + 1]^\beta \quad (V), \quad (16)$$

the molecular attenuation $\alpha(p)$ was discussed in Section 2.

Previous work showed that electronic resolution of amplitude changes to about 0.5% and of frequency changes to about 10^{-3} of the bandwidth ν_R/Q are possible. Hence,

$$\alpha_{\min} \geq 460 \nu_R/Q = 0.022/L_R \quad (\text{dB/km}) \quad (17)$$

and

$$N'_{\min} \geq 10^3/Q \quad (\text{ppm})$$

where Q is the loaded Q -value, ν_R is in gigahertz (GHz), and L_R is the effective free path length in kilometers (km) (Eq. A5, APPENDIX).

The drift rate of the evacuated spectrometer was below 0.05 ppm/hr, mainly a consequence of good temperature control. Proper operation of the spectrometer is indicated when

$$a_1(p) = a_0 \quad \text{and} \quad N'(p) = N_0 p \quad (18)$$

for a nondispersive, lossless gas such as nitrogen. A constant peak detector output implies stable power over the tuning range; a pressure-proportional phase meter output means that the resonance frequency, ν_R , tracks the tuning, $\nu_R(1 - N^0 p)$. Equation (17) emphasizes the importance of achieving a high loaded- Q value for the spectrometer cell. The Fabry-Pérot resonator depicted in Figure A2 has an experimental value of $Q = 258,000 \pm 5$ percent at 35 GHz, equivalent to an effective free-space length of (Eq. A5) $L_R = 0.352$ km.

Typical output signals for the noise and drift levels of attenuation and refraction detection are shown in Figure 3. A simulated attenuation of 0.15 dB/km is clearly distinguishable, while the refraction output is not affected, which is actually true up to $\alpha \approx 20$ dB/km. The minimum detectable signals are estimated to be

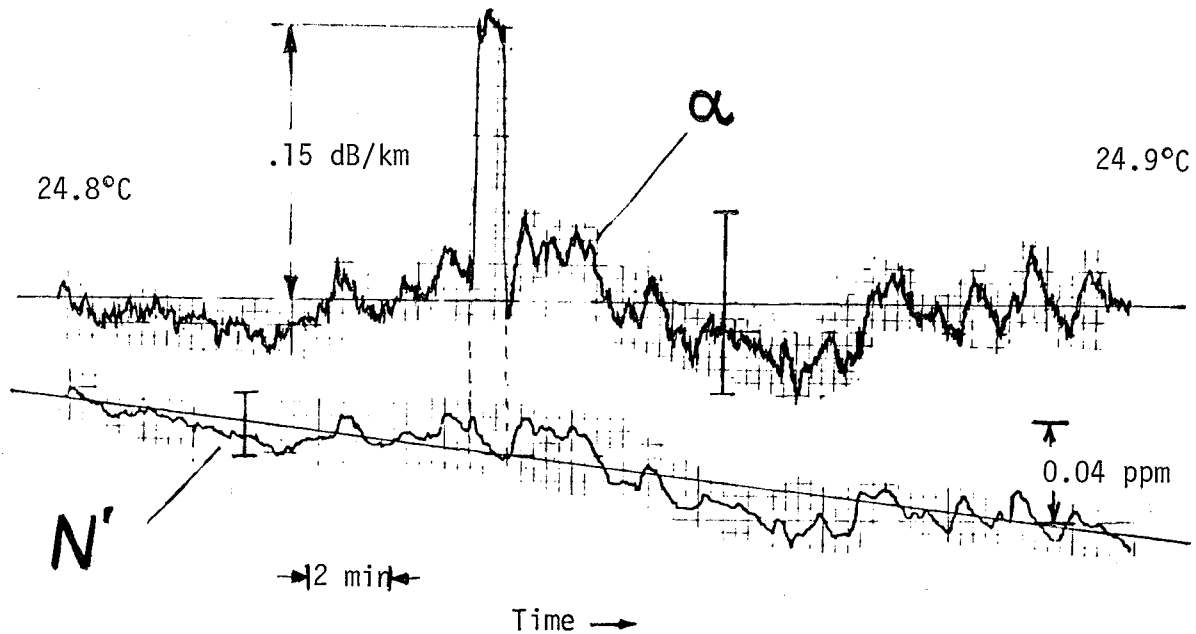


Figure 3. Time series of minimum detectable attenuation and refractivity ($f_T = 1$ kHz, 10^3 samples: $\tau = 1$ s; for other experimental conditions, see Figure 4).

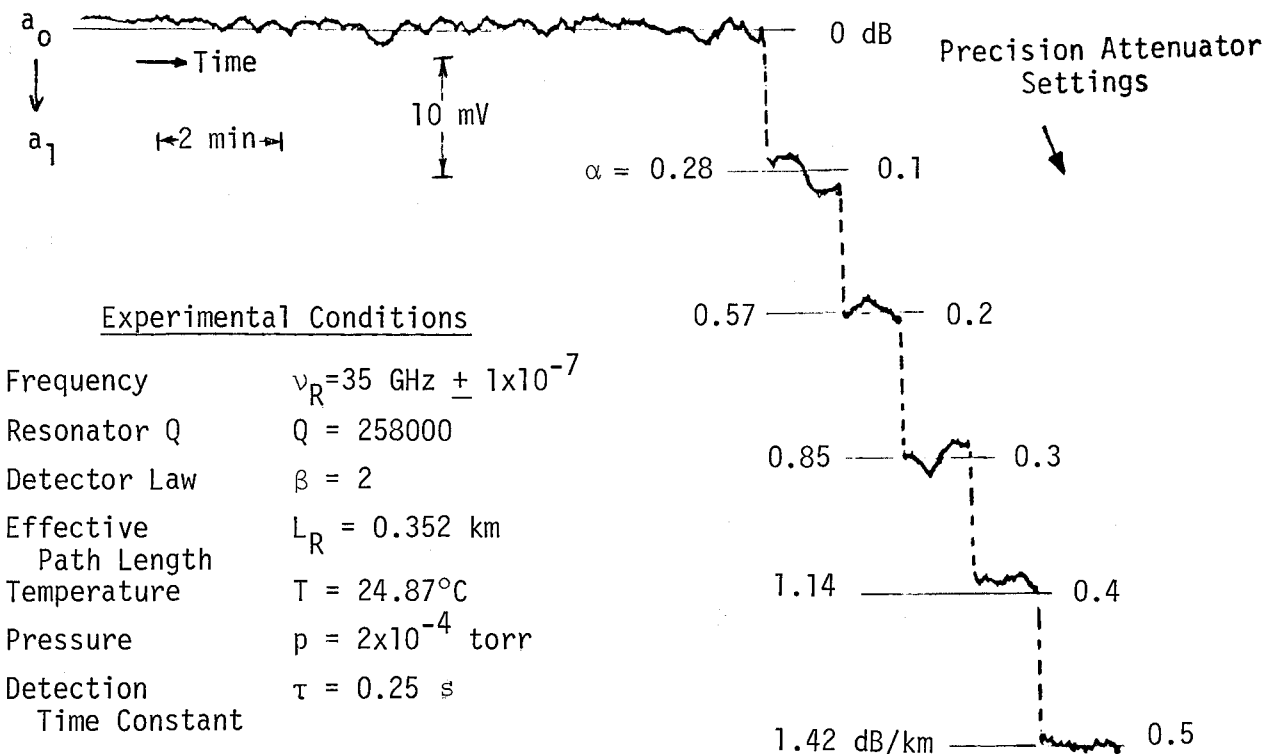


Figure 4. Simulated absorption (see PA_1 in Figure A1) for absolute attenuation calibration α (dB/km).

$$\alpha_{\min} = \pm 0.05 \text{ dB/km.}$$

and

(19)

$$N'_{\min} = \pm 0.01 \text{ ppm.}$$

The refraction time series displays a slight drift, due to changes in temperature, which is negligible since the expected signals are in the range $N' = 1$ to 50 ppm.

The suggested measurement procedure was to measure first at low pressure ($p = 3 \times 10^{-2}$ to > 50 Pa) absorption by the pure species and then proceed to high pressure [$P = p + p_1(N_2)$] scans (1 to 100 kPa) using nitrogen as the host gas and keeping the partial absorber pressure constant at 0.1, 1, 10, and 50 Pa. The accuracy of measurements of the latter kind depends upon a stable absorber concentration. Also, it was always assured that there was no power saturation of the molecular absorption by the measuring field. The microwave power was reduced in cases when absorption was detected to verify that the effect was not power dependent.

3.3 Intensity Calibration

The spectrometer was tuned to frequencies around 35 GHz. The detector was operated at mV levels as a square law ($\beta = 2$) device, defining the halfwidth ν_R/Q of the resonance curve at 1/2 of its peak value. Knowing the Q value, and thereby the effective path length L_R (Eq. 5A), simplifies the calibration of the attenuation scale with a precision attenuator that reads directly in decibels. A typical example of this procedure is illustrated in Figure 4.

Absolute refraction can, in principle, be calibrated by a measurement of dwell time, d , and ν_R (Eqs. A7 and A8), but an indirect method was preferred. Nitrogen refractivity-vs.-pressure recordings (R2 remains evacuated) are linear functions which are easily least-squares-fitted. In this way, the tuning expected from the gas is simulated from the spectrometer cell to the data output.

4. GAS HANDLING

The concentration of the species and the potential danger of degradations of the test cell components needed careful evaluation so that the requirements specified in Table 2 could be met. Two modes of operation were planned:

- (a) Pure vapors are evaporated into the evacuated cell and then mixed with N_2 , based upon pressure measurements. Premixing in the spherical 12ℓ Pyrex chamber to dilute the hazardous vapor with inert N_2 and subsequent injection into the cell is an option for this mode (see Figure 5).

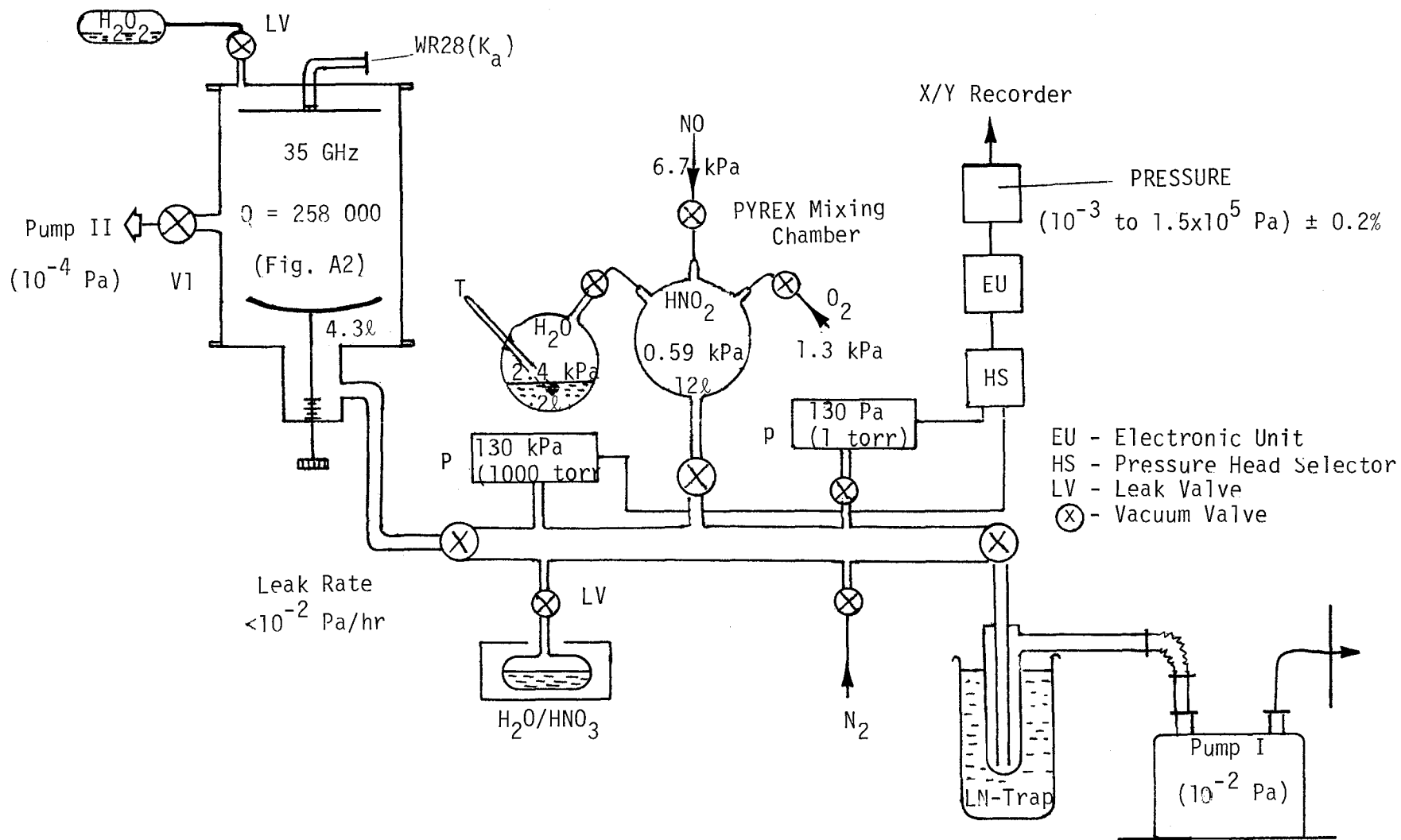


Figure 5. Schematic of gas handling system.

(b) A flow system is employed where N_2 is filtered through the liquid phase of the test gas and is allowed to saturate (e.g., Figure 6) at the pressure commensurate with the temperature of the container.

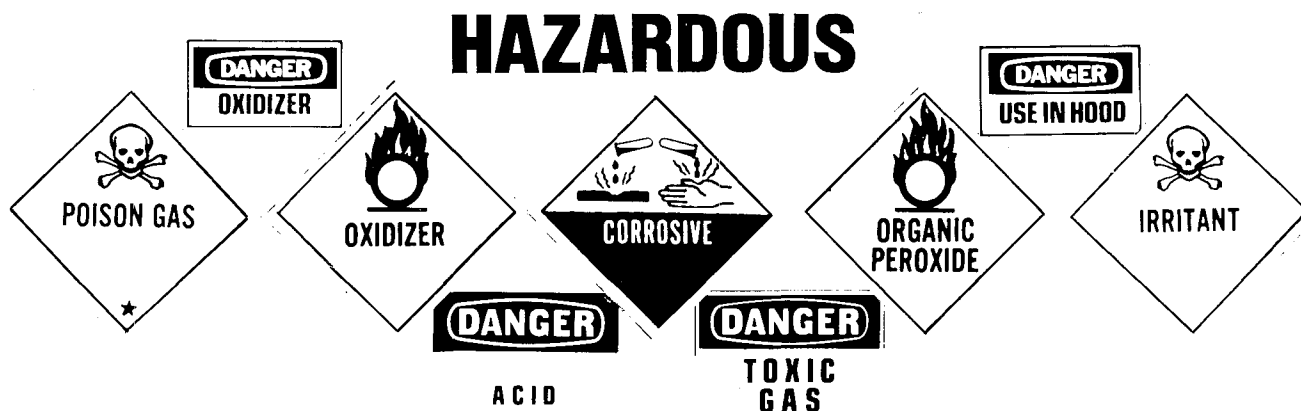
The concentration of absorber molecules in the test cell is subject to errors. The system was checked with a He mass detector and found free of leaks; the outgassing rate stayed below 1×10^{-2} Pa/hr after overnight pumping. The main experimental variable (that is pressure) was measured with a capacitance manometer (MKS) designed for high corrosion resistance and covering the range 10^{-5} to 10^3 torr \pm 0.2 percent with two sensor heads. The calibration was periodically checked in the 10 to 800 torr range against an NBS-traceable standard (RUSKA test gauge 3512, quartz bourdon tube). The ultimate pressure reached with a two-stage forepump and a liquid nitrogen (LN) trap was about 3×10^{-3} Pa (1 torr \equiv 133.32 Pa).

The gas handling system shown schematically in Figure 5 was designed for hostile applications. Materials used were Pyrex, stainless steel (SS304), Viton and Teflon elastomers, all resistant to oxidation and acidic deterioration. The test gas was evaporated into the evacuated resonator, which contains highly-polished, silver-plated mirrors that have no resistance to corrosion. Therefore, the residence time of the gas was kept short (less than five minutes)--just as long as was needed to complete scans with increasing and decreasing pressure and display the resulting $\alpha(p)$ and $N'(p)$ values on two X/Y plotters. The Q-value of the resonator was continuously monitored, and no deteriorations of Q were observed in the course of the measurement series.

Each test gas behaved somewhat differently and required different precautions, as discussed below.

4.1 Precautions

For the test molecules, H_2O_2 , HNO_3 , HNO_2 , and NO_2 , the following precautional labels apply, especially for high concentration in pure form:



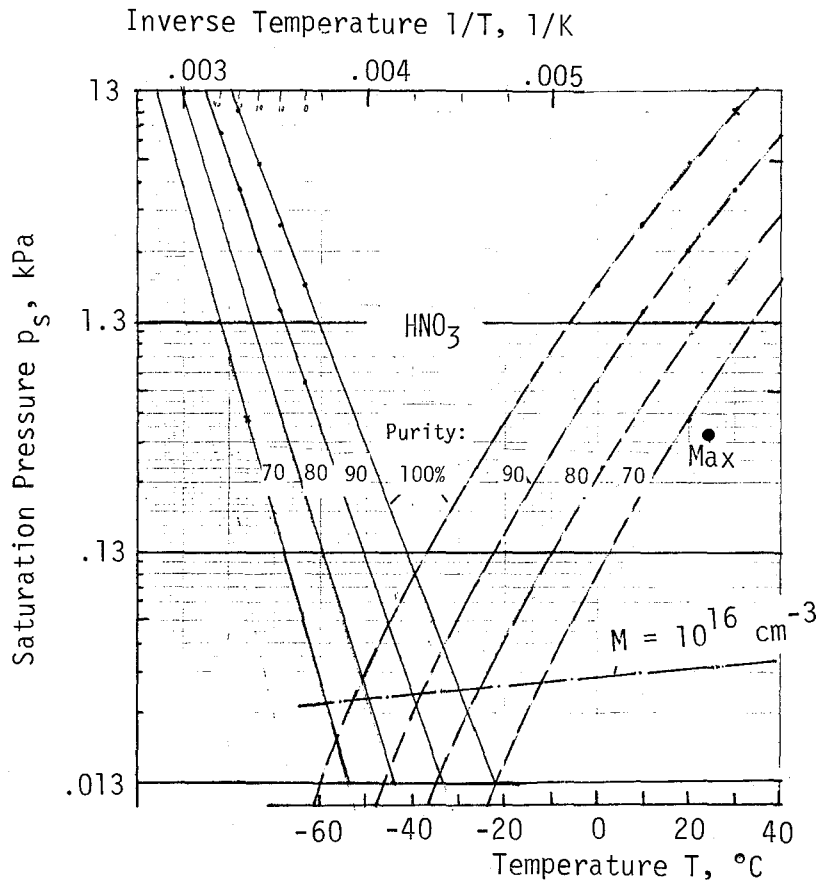


Figure 6. Saturation pressure of nitric acid vapor for different liquid purities (aqueous solution at 68%).

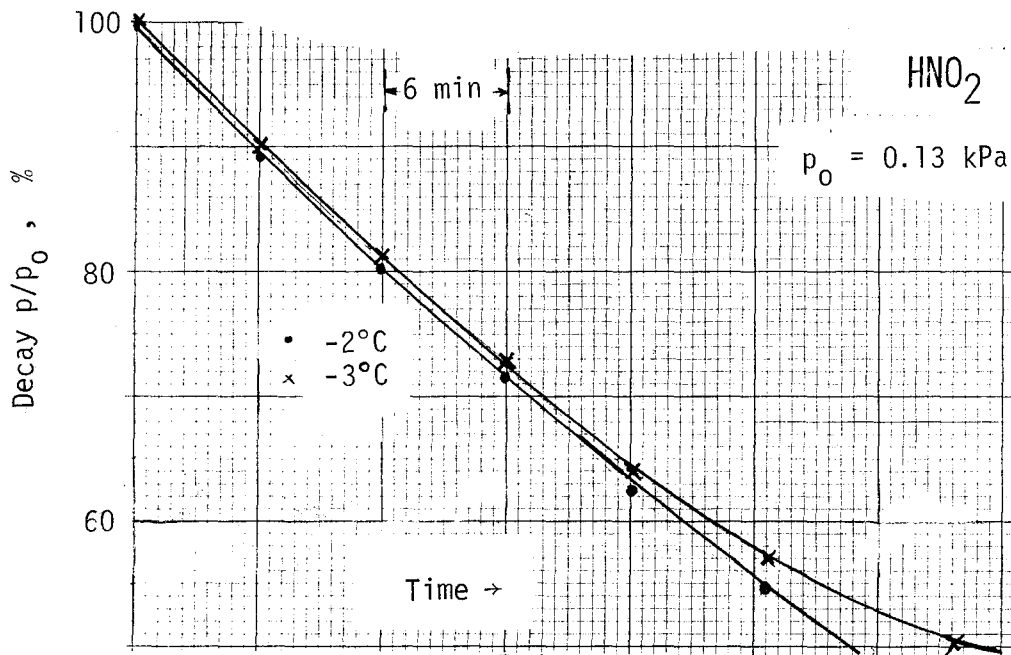


Figure 7. Decay of nitrous acid vapor concentration inside 12 liter Pyrex mixing chamber (see Fig. 5) [J. S. Wells, NBS, private communication, 1980].

The proper equipment and the proper techniques must be used in handling the test species safely. Fume protection with good ventilation, safety glasses, and spill protection with gloves were considered adequate safeguards.

HYDROGEN PEROXIDE (H_2O_2) is a very strong oxidant and should not be allowed to contact organic materials. It is extremely dangerous if even traces get into the eyes. The liquid container needs to be vented to prevent an explosion due to pressure build-up of the decomposing liquid ($H_2O + O_2$). Purification to better than 90 percent is accomplished by extensive pumping on the liquid and trapping the pumped gas at liquid nitrogen temperature. The degree of purity can be checked by a vapor pressure measurement as demonstrated in Table 3 (FMC, 1969)--the purer the H_2O_2 liquid the lower the pressure. A mole fraction of 0.9 in the liquid phase results only in a 0.65 (25°C) mole fraction for H_2O_2 vapor; curves presented in the FMC (1969) handbook can be consulted. In the presence of metal surfaces, gaseous H_2O_2 decomposes rapidly into water and O_2 ; when the surfaces are covered with clear lacquer however, this process is inhibited (Millen, 1960). The decomposition is much slower at pressures well below saturation (< 25 Pa) (Hunt et al., 1965). Detailed spectroscopic measurement techniques are discussed by Oeleke and Gordy (1969).

Table 3. Maximum Vapor Pressure of Liquid $H_2O_2 - H_2O$ Mixtures

Aqueous H_2O_2 :	0	50	80	90	100%
	Ps		kPa		
20°C	2.33	0.893	0.352	0.252	0.181
25°C	3.16	1.23	0.495	0.359	0.230
30°C	4.34	1.65	0.685	0.503	0.369

NITRIC ACID (HNO_3) vapor was taken from a reagent grade (80%) liquid stored in the dark. The saturation pressure for different purities of the liquid and temperatures is given in Figure 6. In this case, the purer the liquid the higher the pressure. The vapor is highly corrosive, and a brief residence time in the unprotected spectrometer cell was important (< 5 min). At pressures above 50 Pa, wall adsorption was observed which required several hours of pumping to restore the original vacuum. The HNO_3 vapor was mixed with N_2 using the system sketched in Figure 5. Experience in handling HNO_3 for spectroscopic studies is reported by Millen and Morton (1960), Brockman et al. (1978), Streit et al. (1979), and Maki and Wells (1980).

NITROUS ACID (HNO_2) vapor generation in pure phase was not accomplished. Concentrations of HNO_2 were attempted with the mixing recipe ($2.4 \text{ H}_2\text{O} + 6.7 \text{ NO} + 1.3 \text{ O}_2$) kPa (see Figure 5). A yield of 0.59 kPa HNO_2 or 7 percent in the ensuing mixture with 8.8 kPa total pressure was calculated, and a rapid decay of the HNO_2 concentration was measured at infrared frequencies exclusively responsive to HNO_2 absorption (Figure 7). The mixture was transferred into the resonator within 10 minutes and pressure scans of $\alpha(p)$ and $N'(p)$ were recorded up to $p = 500 \text{ Pa}$. No absorption, however, was detected. Spectroscopic studies involving HNO_2 in various other mixture combinations are reported by Varma and Curi (1976) and Streit et al. (1979).

NITROGEN DIOXIDE (NO_2) came from a lecture bottle and was calculated to be 99 percent pure at 25°C and $p \leq 150 \text{ Pa}$. The gas is a serious health hazard in air at concentrations above 100 ppm. Measurements with $p \leq 100 \text{ Pa}$ were performed and afterwards the gas was collected in the LN trap.

NITROUS OXIDE (N_2O) or "laughing gas" came from a gas bottle in pure form and behaved like a common gas.

4.2 Measurement Strategy

Attenuation measurements were conducted at room temperature in two steps, each repeated several times. First, a pressure scan of the pure gas was recorded with $p \leq 150 \text{ Pa}$ to detect absorption from lines close to three test frequencies (see Eqs. 2,9,13) and from Debye effects (Eq. 14). Next, the species X under various constant pressures p were diluted with nitrogen and absorption of the mixture $X(p) + \text{N}_2(P)$ was tracked up to $P \leq 100 \text{ kPa}$. This mode probed for possible strong, more distant lines blended together by foreign-gas-broadening (see Eq. 15). Simultaneously with $\alpha(p,P)$, a recording of $N'(p,P)$ was made, and both were displayed on separate X/Y plotters. The refractivity slope $N'/p(P)$ indicated that the test gas had actually entered the resonator, how much was being adsorbed on the cell surfaces, and how stable the gas phase stayed. Amplitude (α) and phase (N') signals are highly correlated (see Figure 3) and runs with anomalous trace behavior could be discarded.

5. RESULTS AND DISCUSSION

The experiments rarely yielded measurable attenuation for the conditions cited in Table 2. In an effort to obtain more interesting data, the following tests were added:

- (a) the concentration limit $M \leq 10^{16} \text{ cm}^{-3}$ was, when safe, exceeded;
- (b) water vapor behavior was studied and compared with already existing data;
- (c) the specific refractivity N'/p was measured;

(d) the molecular dipole moment μ of N_2O was determined from the temperature dependence of N'/p .

5.1 Water Vapor (H_2O)

The measurement series were started using water vapor. For H_2O , a fairly complete theoretical spectrum was at hand, and some of the analytical tools developed in Section 2 could be applied to better appreciate the complexity of problems encountered when discussing $\alpha(AIR + H_2O + X)$. At 35 GHz, water vapor is the most important absorber in normal moist air. The complete rotational spectrum ($J = 0$ to 16) with 2300 lines between 22 GHz and 35 THz is known and was recently re-evaluated (M. Mizushima, private communication, 1981). Strong absorption lines ($\alpha_0 > 10^3$ dB/km) are predicted to fall in the frequency range 0.56 to 16 THz, their number being roughly $i \approx 200$. The low frequency wings of these lines contribute a continuum absorption which is approximated by

$$N'_C \approx 2\nu \sum_i (\gamma S / \nu_0^3)_i \quad (\text{ppm}) \quad (20)$$

Attenuation α and refraction N' by pure water vapor had been measured by us in the past under a variety of conditions (i.e., $\nu_R = 22$ to 75 GHz, $T = 290$ to 318 K, $p \equiv e = 0$ to 7 kPa). Quite similar results were obtained at 35 GHz, as displayed in Figure 8. This self-broadening case yields theoretically with (3) and (20)

$$\alpha_C \approx 0.36 \nu^2 e^2 \sum_i (\gamma^0 S^0 / \nu_0^3)_i \quad (\text{dB/km}) \quad (21)$$

The invariable line sum is estimated from the absorption data (Figure 8) to be $\sum_i (---)_i \approx 3 \times 10^{-5} \text{ GHz}^{-1} (\text{kPa})^{-2}$ at $T = 24^\circ\text{C}$.

In moist air, foreign-gas-broadening dominates, which leads with (20) and the assumption $\gamma = 0.2\gamma^0 P$ to the far-wing contribution

$$\alpha_C \approx 0.36 \nu^2 e (0.2P + e) \sum_i (---)_i \quad (\text{dB/km}). \quad (22)$$

Attenuation measurements in moist air (Liebe, 1980) project a value for the line sum of $\sum_i (---)_i \approx 5.1 \times 10^{-6}$. The discrepancy by a factor 6 between pure H_2O (Eq. 21) and moist air (Eq. 22) attenuation, as well as the correct theoretical value, are currently being investigated.

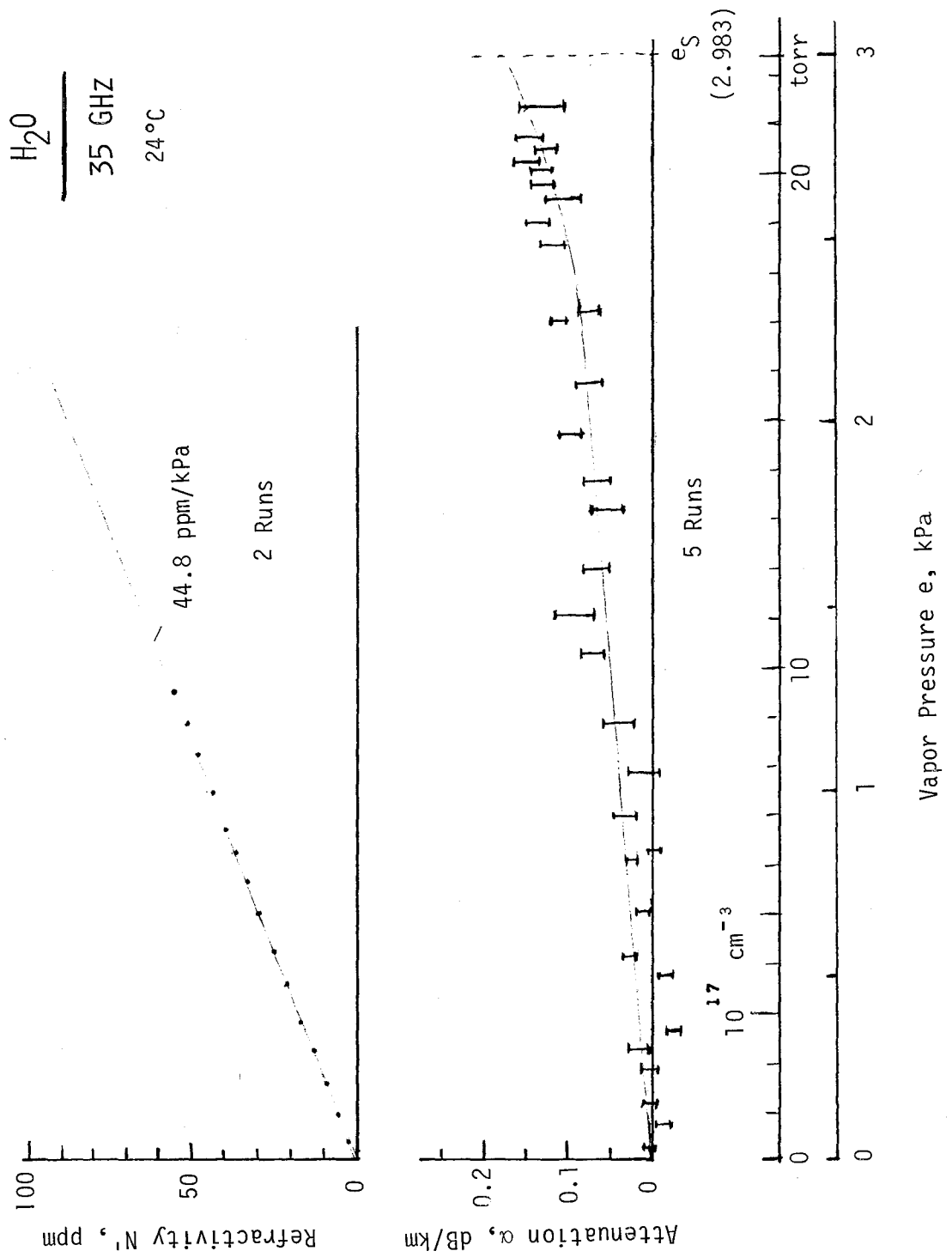


Figure 8. Water vapor attenuation α and refractivity N' at 35 GHz as a function of the vapor pressure e at room temperature.

5.2 Hydrogen Peroxide (H_2O_2)

The results for measurements of hydrogen peroxide (evaporated from a 90 percent pure liquid) are depicted in Figure 9 for increasing and decreasing vapor pressure p . Apparently during the vapor filling of the resonator, some decomposition and wall adsorption took place. The attenuation data display a behavior predicted by (21) with no strong local line contribution. The complete spectrum of H_2O_2 and its line intensity data were not available.

Measurements on binary mixtures $\text{H}_2\text{O}_2 + \text{N}_2$ with $P = 80$ kPa and $p = 0.5, 1,$ and 1.6 kPa produced no measurable attenuation.

5.3 Nitric Acid (HNO_3)

Attenuation and refraction results by nitric acid (evaporated from a 80 percent pure liquid) are shown in Figure 10. Only one run up to $p = 0.33$ kPa was performed because a corrosive attack on the resonator mirrors was feared. At pressure $p > 0.1$ kPa a substantial build-up of adsorbed HNO_3 is noticed in the refraction data, which could be pumped off after some time (two hours). The pure vapor phase exhibited no measurable attenuation for $p \leq 200$ Pa.

Measurements on mixtures of $\text{HNO}_3 + \text{N}_2$ gave the attenuation estimates summarized in Table 4. Again, no clearly measurable attenuation was evident. A response of the 35.110 GHz line (Table 1) was not seen at $\nu_R = 35.00$ and 35.62 GHz, neither in self nor in foreign-gas broadening. The theoretical millimeter wave spectrum of HNO_3 involves several thousand lines (Helminger et al., 1981). Line intensity data were not available.

5.4 Nitrogen Oxides (N_2O and NO_2)

Nitrous oxide (N_2O) gas was easy to work with. It was studied more extensively (36 runs), including a range of temperatures between 12 and 70°C. Absorption was not detected below 5 kPa. The p^2 -dependent absorption above 5 kPa (Figure 11) is indicative either of a far-wing contribution from a line spectrum (Eq. 12) or of collision-induced effects (Eq. 14). The temperature-dependent refractivity data N'/p (Figure 11) were analyzed to determine the molecular dipole moment μ . The results are summarized in Figure 12. Surprisingly, the value $\mu \approx 0.33$ D is about twice the value used in spectroscopic line studies (see Table 1).

Nitrogen dioxide (NO_2) was studied at low pressures ($p \leq \text{Pa}$) and room temperature (24.3°C). At the frequencies of 35.00 GHz and 35.61 GHz, no measurable absorption was detected.



35 GHz

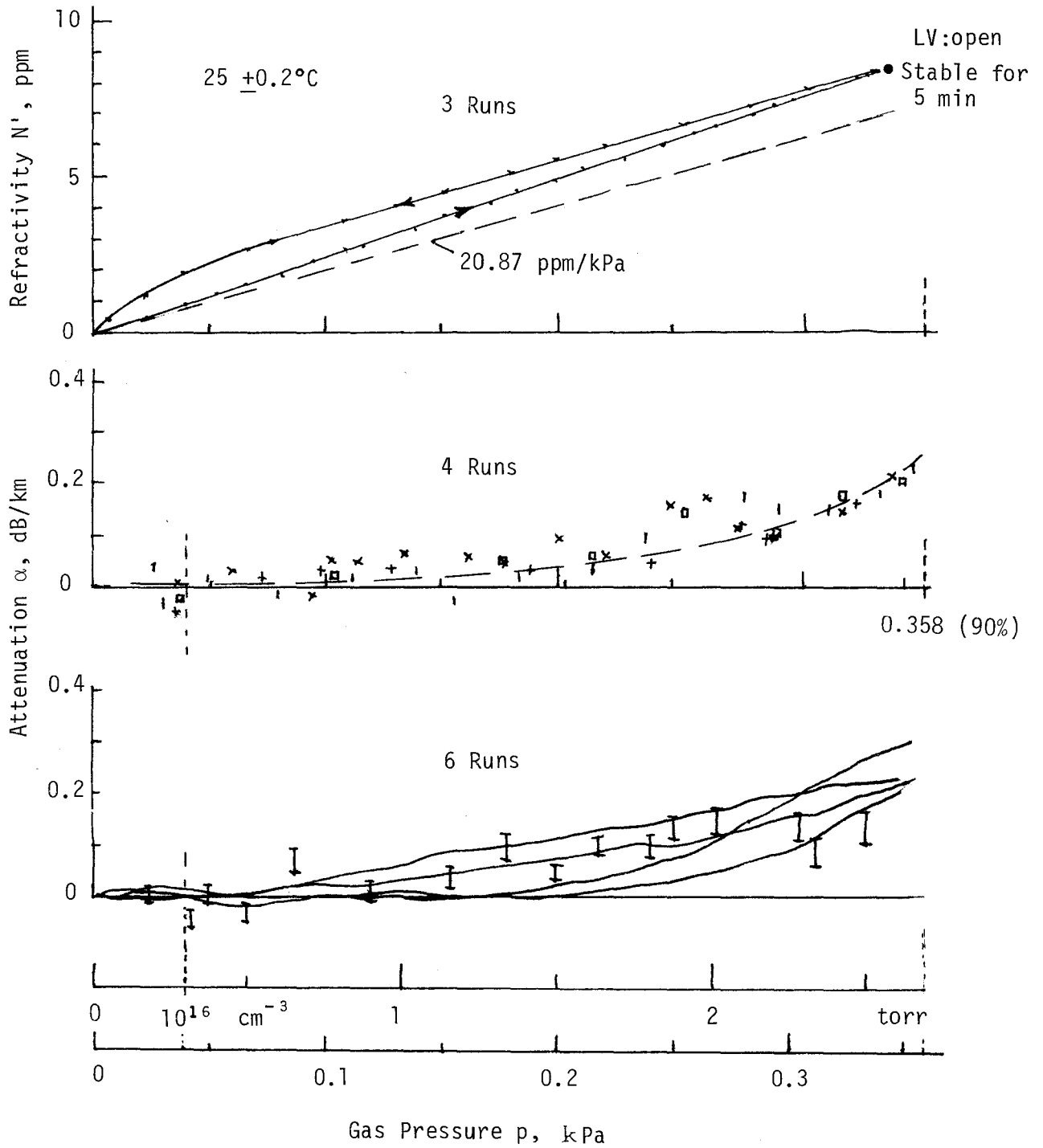


Figure 9. Gaseous hydrogen peroxide attenuation and refractivity at 35 GHz as a function of pressure (90% liquid purity--see Table 3) at room temperature.

HNO₃

35 GHz

25 °C

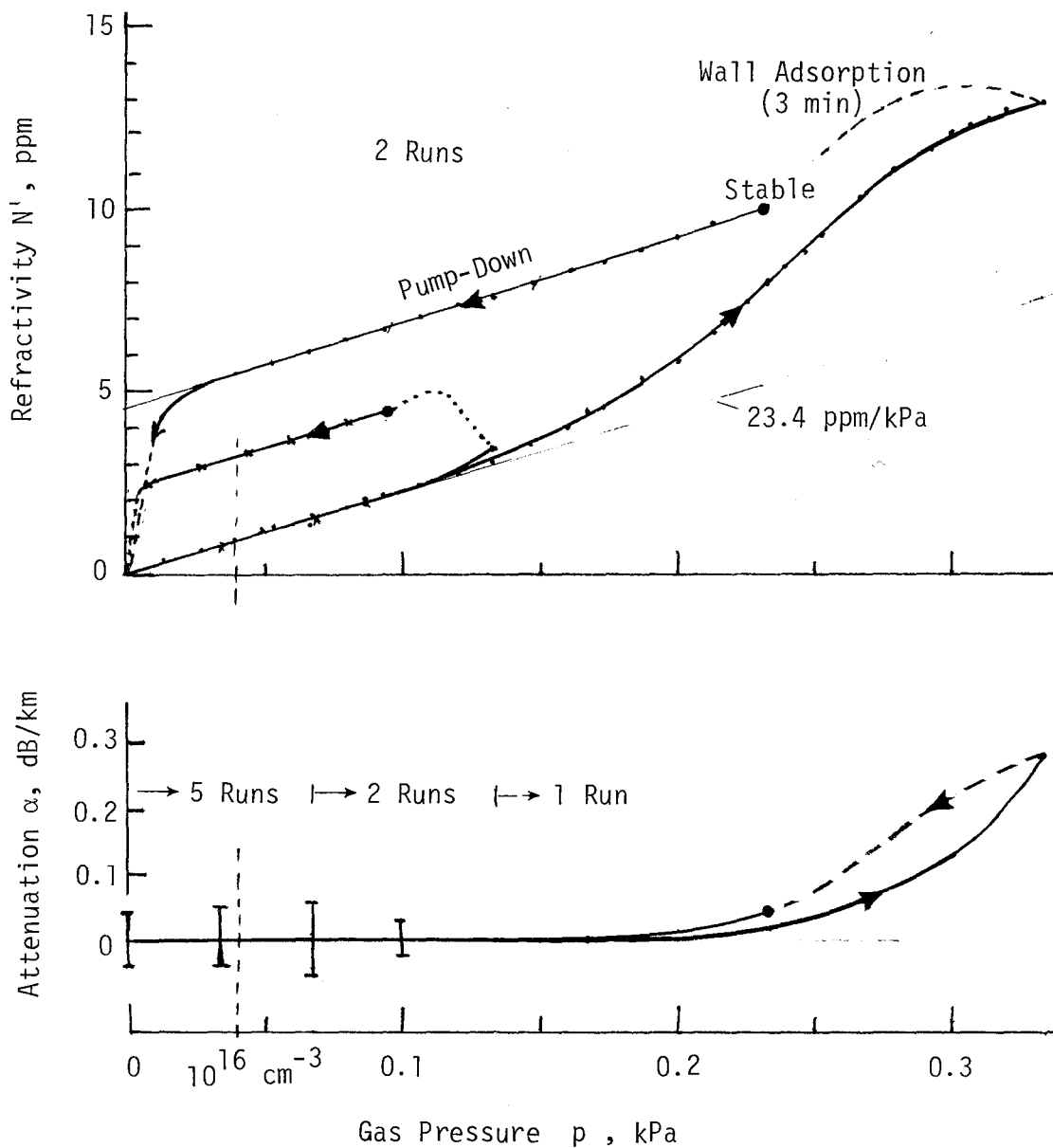


Figure 10. Gaseous nitric acid attenuation α and refractivity N' at 35 GHz as a function of pressure (80% liquid purity--see Figure 6) at room temperature.

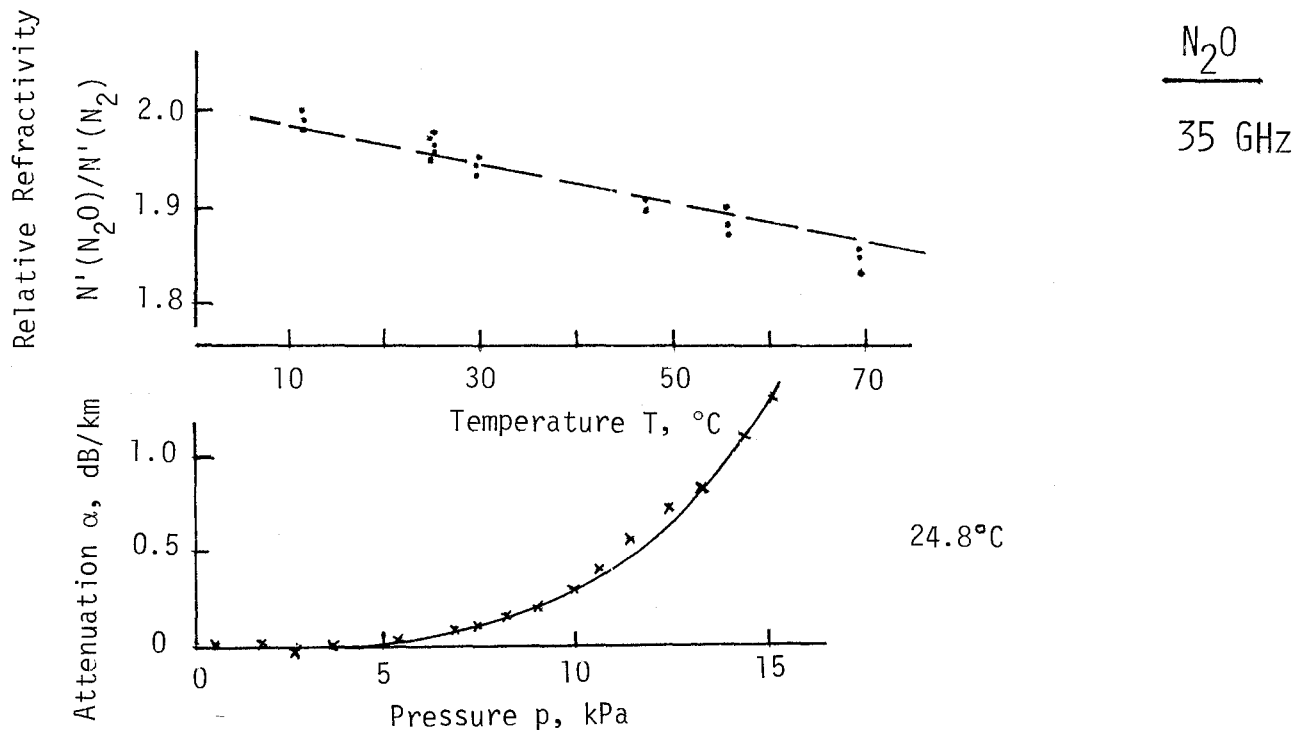


Figure 11. Nitrous oxide attenuation α and relative refractivity $N'(N_2O)/N'(N_2)$ at 35 GHz as a function of pressure and temperature (10 to 70°C).

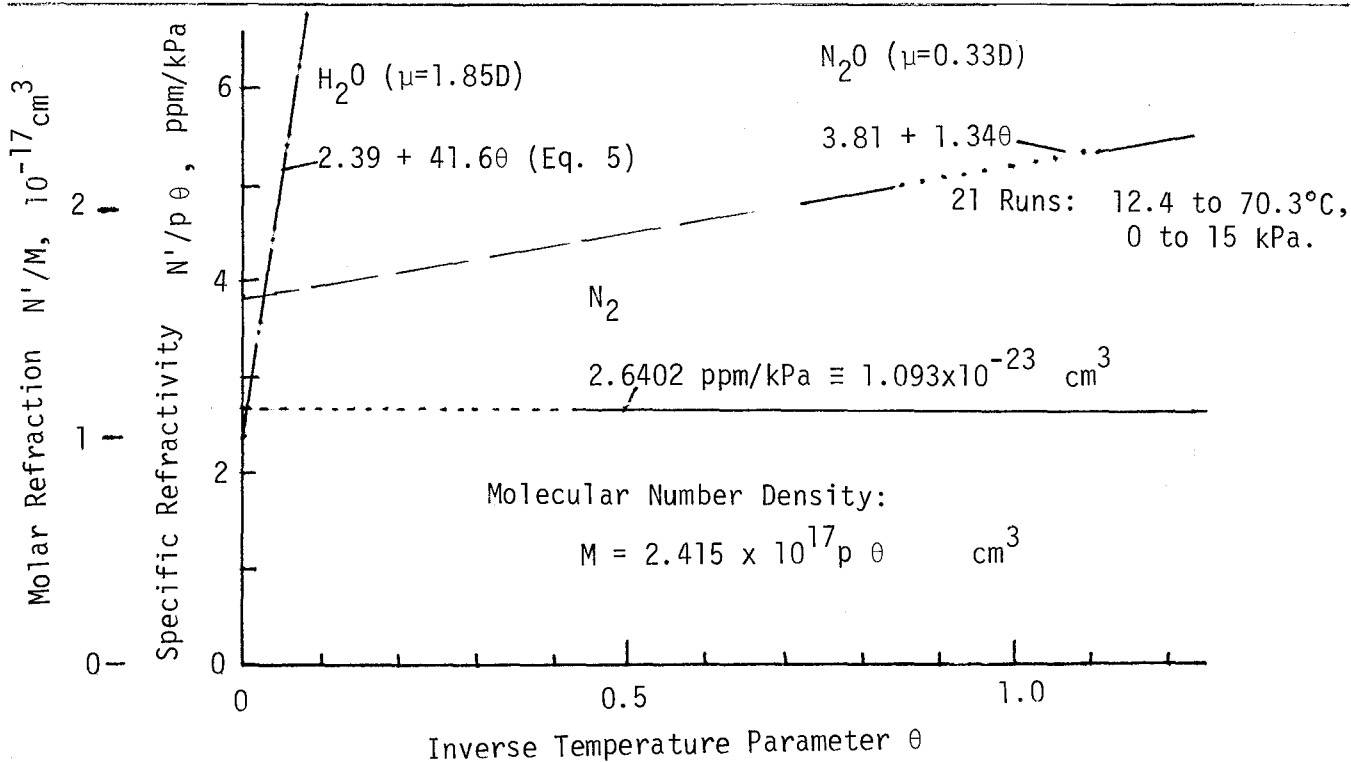


Figure 12. Determination of the molecular dipole moment μ of nitrous oxide.

Table 4. Attenuation by Nitrogen with Traces of HNO₃
 (ν_R = 35 GHz, T = 25.2°C)

HNO ₃	N ₂		Attenuation	Remark
p	P	p/P	α	
Pa	kPa	ppm	dB/km	
0	98.4	0	0	
1.4	67.2	21	0 + 0.05	a)
5.8	69.2	84	0.05 + 0.05	a)
6.3	100.4	63	0.05 + 0.05	b)
12	67.6	178	0.1 + 0.05	b)
13	99.8	130	0.1 + 0.05	b)
37	99.1	373	0.2 + 0.1	b)

- a) Premixing in 12 l Pyrex container (Figure 5).
 b) Mixing in 35 GHz resonator

In Summary--absorption measurements at 34.73, 35.00, and 35.62 GHz with the molecules H₂O₂, NH₃, and NO₂ did not turn up attenuation rates exceeding 0.25 dB/km at room temperature and specified test conditions (Table 2). The tests were performed with fairly pure vapors at low pressures (p < 100 Pa) and for diluted conditions at atmospheric pressures (P < 100 kPa). Whatever little attenuation was measured is suspected to be mostly instrumental effects such as condensation on the spectrometer cell surfaces. Two molecules with absorption lines close to 35 GHz are C₂H₅CN and CH₂HN (Poynter and Pickett, 1980), which are probably inconsequential for the case at hand. This preliminary study provides some certainty for modeling the 35 GHz attenuation in sea level air by considering only H₂O and O₂ (see Section 6). More careful measurements require a corrosion resistant cell construction. All inner surfaces have to be treated with films of silicon or Teflon and an all-glass manifold needs to be employed.

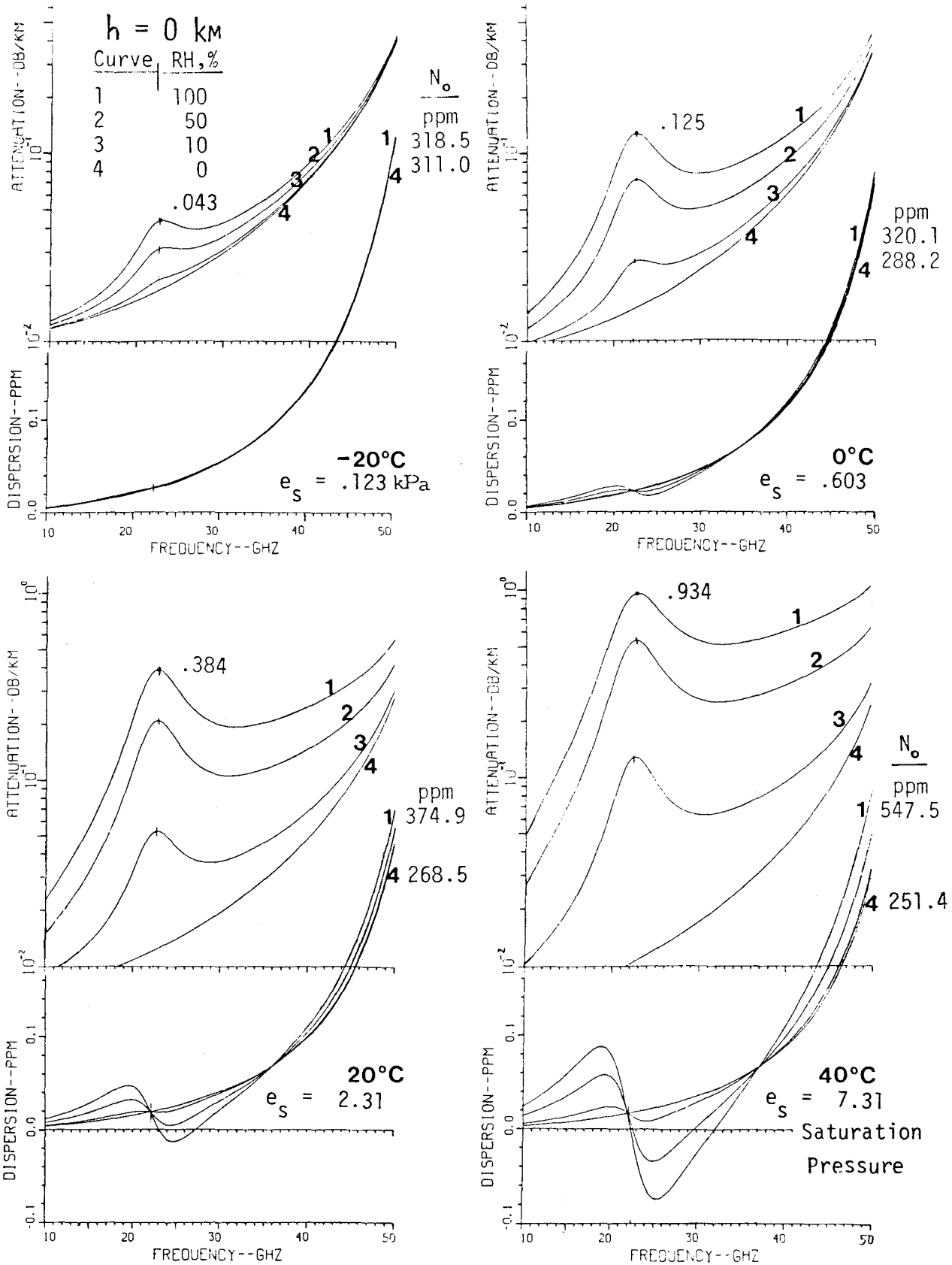


Figure 13. Attenuation predictions (SETPLOT) for moist air at sea level over the frequency range 10-50 GHz at four temperatures between - 20° and 40°C.

6. MODELING

A computer program, SETPLOT, with an associated plotting routine, generates attenuation α (dB/km), refractivity N_0 , and refractive dispersion D (ppm), for any desired resolution over the height range $h = 0$ to 100 km (Liebe, 1981). The range $h = 0$ to 30 km requires as input variables pressure, $p(h)$; temperature, $T(h)$; and relative humidity, $RH(h)$. The spectroscopic data base consists of three parts: (a) resonance information for 44 O_2 and 30 H_2O lines in the form of intensity coefficients and center frequency for each line; (b) an empirical water vapor continuum spectrum; and (c) a liquid water attenuation term for haze conditions. The overlap problem of the 60 GHz oxygen band is taken into account. The program also calculates the Zeeman splitting of O_2 lines over the height range $h = 30$ to 100 km, in which case the earth's magnetic field strength H at a given geographic location becomes an additional input variable.

Automated graphical and numerical output like that of SETPLOT is at the hub of all millimeter wave propagation problems through the clear atmosphere. SETPLOT gives an opportunity for fast and accurate computations of absorption and delay effects with the aid of simple interactive computer instructions for printing and plotting. The confidence limit below 120 GHz, based on extensive data from laboratory studies, is better than four percent.

6.1 Sea Level Behavior of Normal Moist Air

Figure 13 exemplifies the influence of molecular H_2O and O_2 absorption upon the transfer properties of sea level air around 35 GHz for temperatures ranging from arctic (-20°C) to tropical ($+40^\circ\text{C}$) conditions. The pollutants studied (see Table 1 and Section 5) do not add any measurable attenuation (< 0.1 dB/km) to these results, even if their concentration is extremely high (i.e., 10^{16} cm^{-3}).

6.2 One Atmosphere of Hot Air

The SETPLOT program with O_2 and H_2O lines up to 1000 GHz was run at elevated temperatures to predict the properties of heated air. The graphical output is depicted in Figure 14. Oxygen lines with high rotational quantum numbers (> 15) increase the attenuation at 35 GHz when the temperatures exceed 400°K .

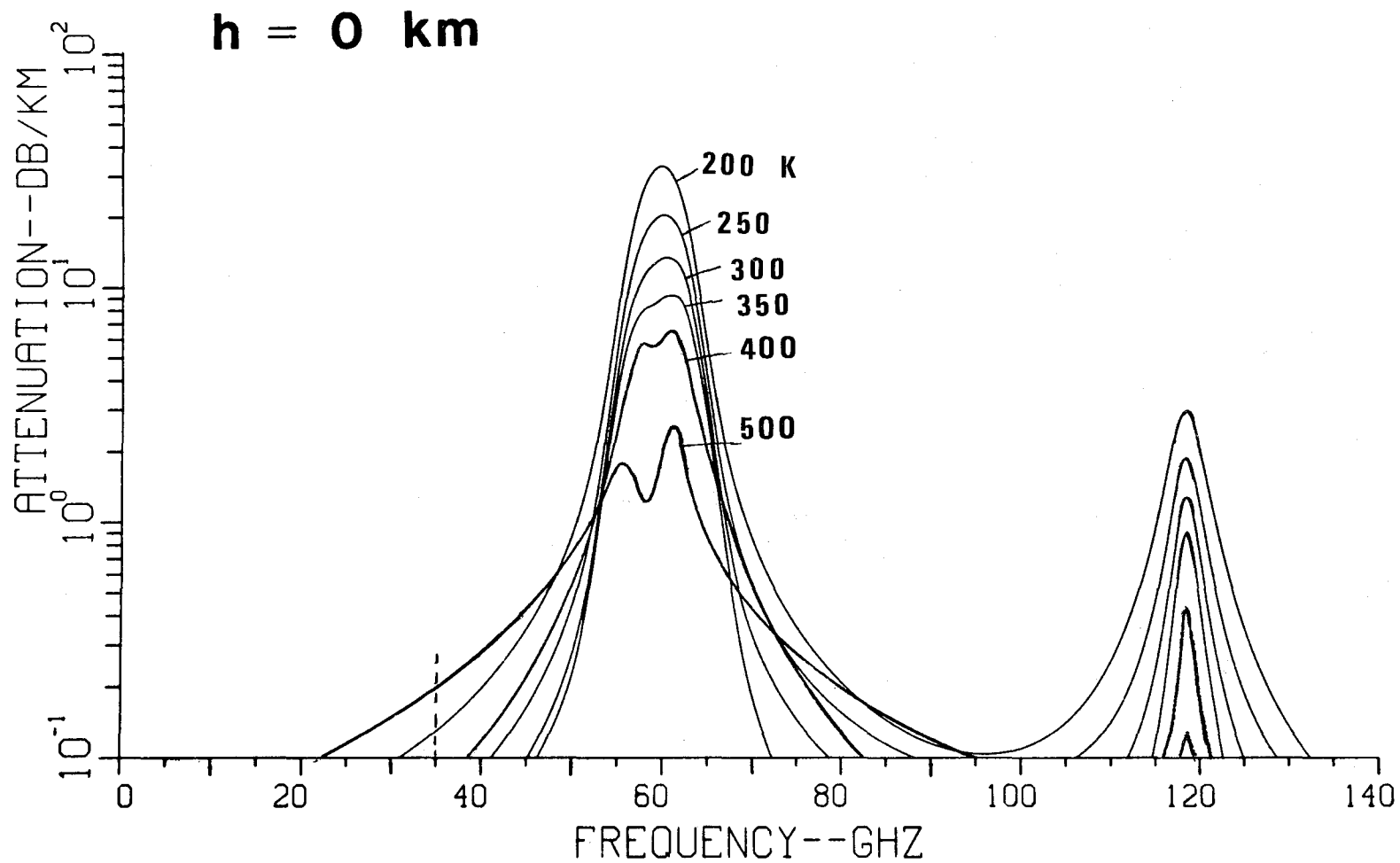


Figure 14. Attenuation predictions (SETPLOT) for hot air at sea level pressure and constant humidity (10 g/m³) over the frequency range 10-50 GHz and temperatures between 200 and 500 K.

7. CONCLUSIONS

At 35 GHz, even unusually high concentrations (< 200 ppm/vol) of the pollutants H_2O_2 , HNO_3 , NO_2 , and N_2O did not cause absorption in excess of 0.25 dB/km. Spectral line absorption of the trace gases is generally drastically reduced by the dominating foreign gas broadening in 1 atm of air (Eq. 15). Some unanswered questions remain in that we were unable, within the limited time available for this study, to measure with some degree of certainty the highly unstable nitrous acid (HNO_2) either in the self or in the foreign-gas-broadened cases. For each the other trace gases, a higher refractivity with respect to nitrogen served as an indicator that the gas actually had entered the spectrometer cell and suggested how it was behaving inside. A temperature study of nitrous oxide (10 to 70°C) yielded as additional information an estimate of its molecular electric dipole moment.

Model calculations using the SETPLOT routine for moist air and covering climatic extremes with temperatures between -20 and 40°C and relative humidities up to 100 percent (Figure 13) identified H_2O as the dominant absorber in normal sea level air. The H_2O absorption is partly caused by a nonresonant spectrum which is not completely understood (Liebe, 1980). It is, so far, only accounted for by an empirical expression. Further experimental studies are recommended to reveal the true physical origin of this effect, which becomes really important in the higher frequency windows (that is, around 90, 140, and 220 GHz). The modeling results for hot air (Figure 14) show that the O_2 microwave spectrum by itself, neglecting vibrationally-excited lines, is a source of attenuation.

The following suggestions are made to continue this work:

- (1) To prepare an experiment, which measures absorption at 35 GHz by heated oxygen at temperatures up to 700°K.
- (2) To include in the attenuation model (Liebe, 1981) vibrationally-excited absorption lines of oxygen that become important at high temperatures.
- (3) To try various other techniques for producing at room temperature a better defined yield of HNO_2 . For example, mixing NO_2 , NO , and H_2O in the ratio 2:1:1 and using a continuous flow system from the mixing bulb through the spectrometer cell (Bowman et al., 1981a).
- (4) To initiate experimental (ITS has the necessary equipment) and analytical studies in the 90 and 140 GHz atmospheric window ranges. While the pollution effects investigated so far proved to be of little consequence at 35 GHz, the situation might be less favorable at higher frequencies, since absorption increases roughly with frequency squared.

8. REFERENCES

- Bowman, W. C., F. C. DeLucia, and P. Helminger (1981a), Millimeter and submillimeter spectra of $\text{HNO}_2(\text{cis})$, $\text{HNO}_2(\text{trans})$, and HNO_3 , *Molec. Spectros.* 88, 431-433.
- Brockman, P., C. H. Blair, and F. Allario (1978), High resolution spectral measurements of the HNO_3 11.3 μm band using tunable diode lasers, *Appl. Opt.* 17, 91-100.
- Cazzoli, G. H., and F. C. DeLucia (1979), Millimeter-wave spectrum, centrifugal distortion analysis, and energy levels of HNO_3 , *J. Molec. Spectros.* 76, 131-141.
- FMC (1969), Hydrogen peroxide physical properties data book, FMC Corp., NY, NY (3rd Ed.).
- Helminger, P., W. C. Bowman, and F. C. DeLucia (1981), A study of the rotational-torsional spectrum of hydrogen peroxide between 80 and 700 GHz, *J. Molec. Spectros.* 85, 120-130.
- Hunt, R. H., R. A. Leacock, C. W. Peters, and K. T. Hecht (1965), Internal-rotation in hydrogen peroxide, *J. Chem. Phys.* 42, 1931-1946.
- Kolbe, W. F., H. Buscher, and B. Leskovar (1977), Microwave absorption coefficients of atmospheric pollutants and constituents, *J. Quant. Spectros. Rad. Transfer* 18, 47-64.
- Liebe, H. J. (1975), Pressure-scanning mm-wave dispersion spectrometer, *Rev. Sci. Instr.* 46, 817-825.
- Liebe, H. J. (1980), Atmospheric water vapor: a nemesis for millimeter wave propagation in *ATMOSPHERIC WATER VAPOR* (A. Deepak et al., editors), Academic Press, NY, NY, 143-201.
- Liebe, H. J. (1981), Modeling attenuation and phase of radio waves in air at frequencies below 1000 GHz, *Radio Sci.* 16, 1183-1199.
- Maki, A. G., and J. S. Wells (1980), High-resolution measurement and analysis of the infrared spectrum of nitric acid near 1700 cm^{-1} , *J. Molec. Spectros.* 82 427-434.
- Meier, D. (1979), Microwave absorption at 94 GHz by molecular interaction in the system $\text{H}_2\text{O}-\text{SO}_2$, *Advances in Molec. Relaxation and Interaction Processes* 14, 91-98.
- Millen, D. J., and J. R. Morton (1960), The microwave spectrum of nitric acid, *J. Chem. Soc.*, 1523-1528.
- Oeleke, W. C., and W. Gordy (1969), Millimeter-wave spectrum of hydrogen peroxide, *J. Chem. Phys.* 51, 5336-5343.

- Poynter, R. L., and H. M. Pickett (1980), Submillimeter, millimeter, and microwave spectral line catalogue, JPL Publication No. 80-23, Jet Propulsion Laboratory, NASA, Pasadena, CA, June.
- Streit, G. E., J. S. Wells, F. C. Fehsenfeld, and C. J. Howard (1979), A tunable diode laser study of the reactions of nitric and nitrous acids: $\text{HNO}_3 + \text{NO}$ and $\text{HNO}_2 + \text{O}_3$, J.Chem.Phys. 70, 3439-3443.
- Varma, R., and R. F. Curi (1976), Study of the $\text{N}_2\text{O}_3 - \text{H}_2\text{O} - \text{HNO}_2$ equilibrium by intensity measurements in microwave spectroscopy, J.Phys.Chem. 80, 402-409.

APPENDIX. PRESSURE-SCANNING MM-WAVE SPECTROMETER

The cavity spectrometer is a very sensitive instrument (Liebe, 1975) a feature desirable for quantitative work. The instrument measures the dimensionless complex refractivity $N = N' - jN''$ in units of parts per million, which is a macroscopic measure of the interaction between gas molecules and radio waves. Real and imaginary parts are related by the well-known Kramers-Kronig formula. The imaginary part is called extinction and converts to attenuation rate

$$\alpha = 4.192 \times 10^{-5} \nu N'' \text{ (1/cm)} \equiv 0.1820 \nu N'' \text{ (dB/km)} \quad (\text{A1})$$

$$[(4\pi/c) = 4.192 \times 10^{-5} \quad , \quad (4\pi/c) 10 \log e = 0.1820]$$

when the frequency ν is in gigahertz (GHz).

A1. Gas-filled Resonator and Modes of Operation

The complex response curve of a gas-filled resonator is described by

$$a(\nu) \propto \{Q^{-1} + Q_M^{-1} + j2 [(\nu/\nu_R)(1 + N'/10^6) - 1]\}^{-1} \quad (V) \quad (\text{A2})$$

where $a(\nu)$ is the voltage output of a linear detector, Q is the loaded-Q value, ν_R is the resonance frequency of the evacuated resonator; and a Q value of the gas is defined by

$$Q_M = 91\,021 \nu_R / \alpha = 10^6 / 2N'' \quad (\text{A3})$$

$$[(2\pi/c) 10 \log e = 91021]$$

(e.g., $\nu_R = 35$ GHz, $\alpha = 1$ dB/km, $Q_M = 3.19 \times 10^6$).

Two modes of spectrometer operation follow from Eq. (A2) when the evacuated resonator is slowly subjected to increasing gas pressure p (Boudouris, 1963; Newell and Baird, 1965; Vetter and Thompson, 1967):

(a) **ABSORPTION MODE:** To measure α we need one resonator swept across its resonance ν_R . The shape of the response curve, Eq. (A2), appears as a voltage $a(t)$ when rectified with a detection exponent β between 1 and 2. The decrease in the maximum amplitude $a_0(p = 0)$ at ν_R to values $a_1(p)$ is sensed by a peak detector when

the pressure p is varied. The absorption is obtained from

$$\alpha = 4.343 [(a_0/a_1)^{\beta^{-1}} - 1]/L_R \quad (\text{dB/km}) \quad (\text{A4})$$

$$[10 \log e = 4.343]$$

where the effective path length is given by

$$L_R = 4.771 \times 10^{-5} Q/\nu_R \quad (\text{km}) \quad (\text{A5})$$

$$[(c/2\pi) = 4.771 \times 10^{-5}]$$

(e.g., $Q = 2.5 \times 10^5$, $\nu_R = 35$ GHz, $L_R = 0.341$ km).

(b) REFRACTION MODE: To measure N' , we need two swept resonators with vacuum resonances ν_R . When one resonator is filled with gas, its resonance shifts by a small amount to ν_N and the refraction is simply

$$N' = 10^6 [\nu_R - \nu_N(p)]/\nu_R \quad (\text{ppm}). \quad (\text{A6})$$

A2. Spectrometer Design

The main features of a spectrometer operating in the 25-75 GHz band are described here; more details are found in (Liebe, 1974). The objectives are to achieve a resolution of N' to better than 1 part in 10^8 and a stability of ν_R of similar order over the pressure range $p = 10^{-1}$ to 10^5 Pa while the temperature T is kept constant. The block diagram Figure A1 depicts four main instrumental groups:

1. Resonator pair

The gas molecules interact with radiation inside the resonators R1 and R2. Before filling, a standard all-metal vacuum station pumps the system down to less than 1×10^{-4} Pa. A quartz thermometer (0.1° mC resolution) and thermistors (installed inside the gas volume and in the metal structure of the resonators) serve as temperature sensors. The mean temperature is controlled by a bath circulator. **Pressure** is measured by an electronic manometer to better than 0.1%. Two main valves (V1,V2) allow simultaneous or separate charges of R1, R2 with the test gas.

2. Excitation of the spectrometer cells

A klystron supplies about 200 mW in the 27 to 36 GHz band of which a small portion (-20 dB) is used to excite R1. The main power drives a second harmonic

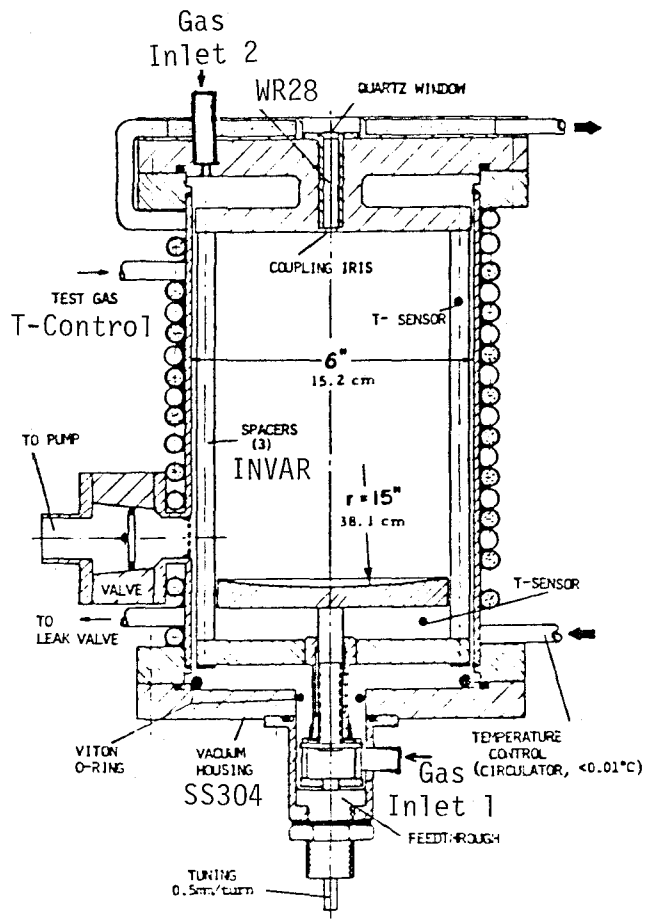


Figure A2. Construction details of the Fabry-Pérot resonator R1 for operation in the 26.5-40 GHz band (drawn to scale).

generator with a conversion loss of about 10 dB to excite R2. The instantaneous bandwidth of the multiplier covers the power mode (~ 100 MHz) of the frequency modulated klystron. The modulator generates positive or negative sawtooth voltages, $\pm u_M$. The repetition rate f_T can be set at 1, 2.5, or 5 kHz, locked to a 5 MHz frequency standard. The klystron dc supply voltages are highly regulated with extremely low ripple (~ 1 mV at 2000 V). An AFC feedback loop ensures that the klystron center frequency coincides with ν_R .

3. Detection of spectrometer signals

The reflected resonator signals are separated with high directivity couplers (>40 dB) and rectified by Schottky-barrier diodes. An FET impedance (high to low) and polarity (- to +) inverter passes the pulse train of resonator responses into a phase meter and also into a peak detector for attenuation measurements. In the reflection (N') mode, a phase meter generates a series of rectangular pulses within the time frame of one FM sweep (see A2.2).

4. Frequency measurement

The test frequency ν_R is measured with a commercial klystron stabilizer. This unit incorporates a ten-crystal base oscillator (15.0 - 15.1 MHz), a multiplier chain to K band ($\times 12 \times 150$ to 180), mixing with the frequency modulated klystron power, and an IF phase detector. Very little residual FM is present at the 2000th order harmonics, allowing a "clean" zero beat with the swept klystron power. Three frequency readings determine the absolute value of ν_R : (a) establishing coincidence either manually or automatically (voltage control of the 15 MHz base oscillator) between the zero-beat and the maxima of the resonator response curves and reading the RF base frequency to about 1 part in 10^7 ; (b) using a frequency meter to estimate ν_C in order to obtain the harmonic number x ; and (c) reading the IF reference of the phase detector. The frequency ν_R is given by $x(\text{RF}) \pm (\text{IF})$. Frequency readout is by a programmable calculator that performs the above calculation on readings from a 50 MHz counter, automatically switched between RF and IF.

A2.1. Resonators

The resonators are most critical and required considerable design effort to assure their performance in the dual role of transmission path and environmental chamber. Two semiconfocal Fabry-Pérot resonators, each with a flat launching and a spherical, reflecting mirror and both of circular shape, are used. Construction details that evolved from the necessity to minimize pressure and temperature influences are evident from Figure A2. Both resonators are one-port reflection

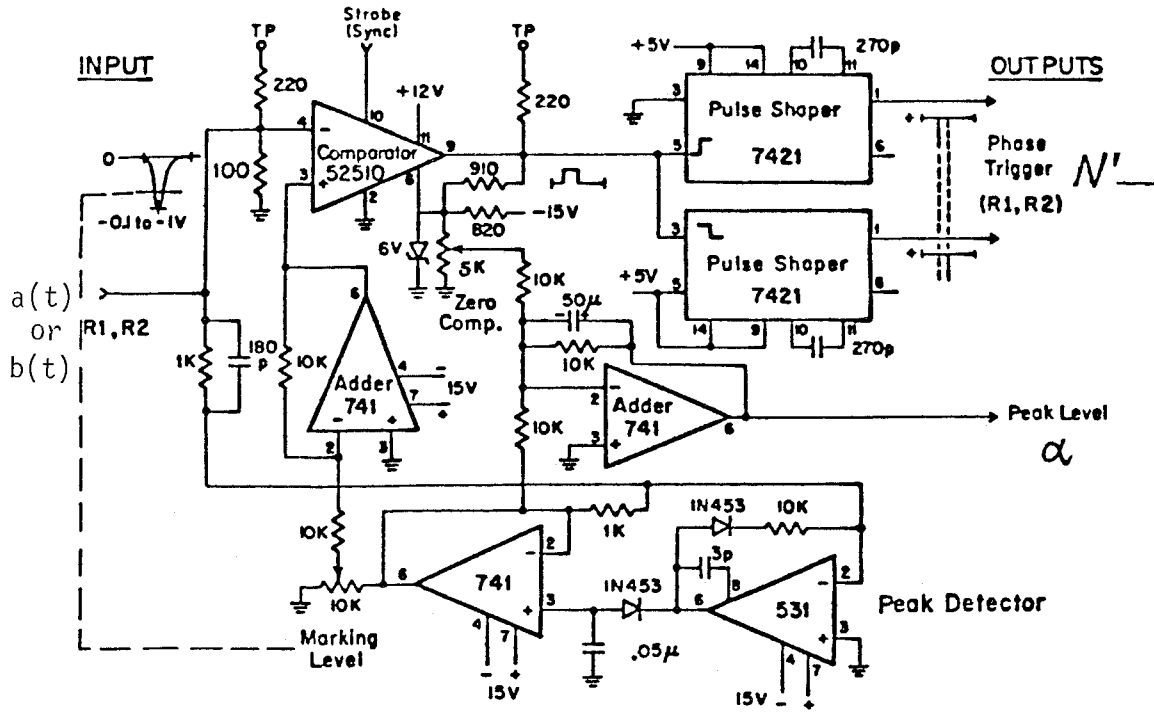


Figure A3. Circuit diagram of phase marker and peak level detector. Two identical channels for v_R and $2v_R$.

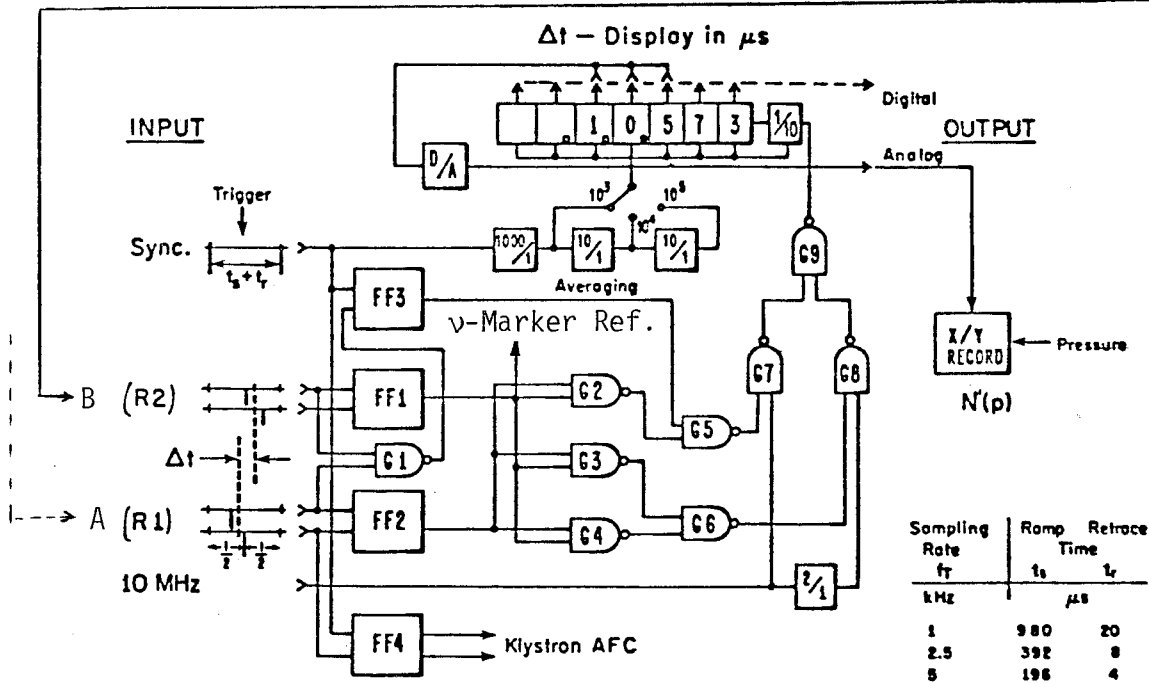


Figure A4. Block diagram of time interval averaging for refraction $N'(p)$.

devices with direct, weak waveguide coupling terminating in an iris. The iris diameters were determined empirically for a 5% dip (a_0) in the total reflected power.

The loaded-Q values were obtained (uncertainty $\leq 5\%$) from the measured bandwidth BW of the reflected signals $a(t)$ and $b(t)$ (Figure A1). Over the tuning range $\Delta l = 2$ cm, eight R2 resonances alternated between the fundamental (TEM_{001}) and the first higher order mode (TEM_{011}). The loaded-Q values of the resonances were between $(2 \text{ to } 4) \times 10^5$.

A2.2. Phase Meter

A sampling phase meter is employed for refraction (N') measurements. Two identical channels accept the resonance pulses a and b (Figure A1).

The data evaluation was improved when compared with [1] by six building blocks:

1. two linear, low-noise preamplifiers for the resonance pulses of R1 and R2;
2. two phase markers and peak detectors for refraction and attenuation measurements (Figure A3);
3. a digital phase meter with time period averaging of dispersion data (Figure A4);
4. a linear ramp generator for \pm klystron FM at rates, $f_T = 1, 2.5,$ and 5 kHz;
5. a time period generator deriving the sweep rate f_T and 0.1 and $0.2 \mu s$ time units from a 1 MHz standard frequency;
6. extremely well regulated power supplies ($+70, +15, +12, +5$ V).

The circuit details are available upon request.

A few of the design ideas that have been incorporated deserve mention. The pulses, which are detected when sweeping the R1(R2) resonance, are amplified in two identical channels to a peak value of $a_0 = -1$ V and fed into a comparator and peak detector (Figure A3). The comparator generates rectangular pulses whose widths correspond to the width of the R1(R2) resonance at a predetermined level, say $0.8a_0$ (variable between 0.1 and 0.99). Leading and trailing edges of each rectangular pulse are transformed into a pair of trigger pulses identified by A_1, A_2 and B_1, B_2 . It is assumed that the resonance frequency $\nu_{R1}(\nu_{R2})$ occurs timewise in the middle between the two triggers. The phase marking is very accurate due to high common gain and low hysteresis of the comparator (~ 1 mV uncertainty).

The decrease of the R2-channel signal amplitude due to molecular absorption from $a_0 \rightarrow a_1$ is tracked by a peak detector, which also keeps the comparator level

constant (present level). This AGC-scheme avoided phase errors otherwise introduced by molecular absorption.

Refraction data are obtained from the time sequence of the triggers, $A_1 - A_2$ and $B_1 - B_2$, within one time frame of the FM sweep marked by $S - S'$. The Δt -measurement is performed by the gating logic (NAD gates G1-G9) shown in Figure A4, which decides Δt automatically between two cases possible in the sequence of triggers:

<u>Case 1</u>		<u>Case 2</u>	
Time Lapse	Count Unit, μs	Time Lapse	Count Unit, μs
$S - A_1$ or $S - B_1$	0	$S - A_1$ or $S - B_1$	0
$A_1 - A_2$ or $B_1 - B_2$	0.2	$A_1 - B_1$ or $B_1 - A_1$	0.2
$A_2 - B_1$ or $B_2 - A_1$	0.1	$B_1 - A_2$ or $A_1 - B_2$	0
$B_1 - B_2$ or $A_1 - A_2$	0.2	$A_1 - B_2$ or $B_2 - A_2$	0.2
$B_2 - S'$ or $A_2 - S'$	0	$B_2 - S'$ or $A_2 - S'$	0

The desired time interval Δt is the total count over one sweep period. The result is displayed as an average of 10^3 , 10^4 , or 10^5 periods. For a sweep width of $\Delta v_M = 2.5$ MHz, the sweep speed can be chosen between $\delta = 2.5$ ($f_T = 1$ kHz) and 13 ($f_T = 5$ kHz) kHz/ μs , while the time for a Δt -reading varies between 0.2 sec ($f_T = 5$ kHz, 10^3 periods) and 100 sec ($f_T = 1$ kHz, 10^5 periods).

A2.3. Signal Processing

The occurrence of the frequencies ν_{R_1} , ν_{R_2} along the time period t_T is marked, transforming the difference between them into a time displacement Δt . Refraction (R2 remains evacuated) is given by

$$N' = \Delta t d / \nu_R \quad (\text{ppm}) \quad (A7)$$

The sweep speed (dwell time) for ν_R ,

$$d = \Delta v_M / t_T \quad (A8)$$

is a basic instrumental constant, where Δv_M is the linear FM sweep width of the klystron (linear within $\pm 1\%$ for a range of 300 ppm for 35 V11 OKI klystron) over a sawtooth duration $t_T = r/f_T$, where f_T is the sampling rate and $r = 0.95$ is the relative ramp time.

Channels A and B drive the output circuits and two AFC loops for frequency marker and klystron center frequency (Figure A1), respectively.

Seven digital outputs [four voltmeters for p , N' , a_1 , and u_M ; two counters for (R_F, I_F) and T ; and a timer for N' (digital)] are connected through a multiplexer to a data-logging system. For on-line analysis, data are transmitted at a slow rate (<1 data pair/sec) to a time-shared computer; for off-line processing, a higher data rate (<50 data pair/sec) can be acquired on magnetic tape. A programmable calculator adds flexibility in initiating various subprograms such as read $v_R(RF,IF)$, calibrate N' by linear least-squares fit of nitrogen refractivity, and read four temperature test points with periodical printout.

REFERENCES FOR APPENDIX

- Boudouris, G. (1963), On the refractive index of air, and absorption and dispersion of centimeter waves by gases, J.Res. Nat'l. Bureau of Standards D67, 631-684.
- Liebe, H. J. (1974), A pressure-scanning refraction spectrometer for atmospheric gas studies at millimeter wavelengths, OT Report 74-35, U. S. Dept. of Commerce, Office of Telecommunications, GPO, Washington, D. C.
- Liebe, H. J. (1975), Pressure-scanning mm-wave dispersion spectrometer, Rev. Sci. Instrum. 46, 817-825.
- Newell, A. C., and R. C. Baird (1965), Absolute determination of refractive indices of gases at 47.7 GHz, J. Appl. Phys. 36, 79-83.
- Vetter, M. J., and M. C. Thompson (1967), Solid state microwave refractometer, Rev. Sci. Instrum. 38, 1726-1727.

BIBLIOGRAPHIC DATA SHEET

1. PUBLICATION NO. NTIA Report 82-96		2. Gov't Accession No.	3. Recipient's Accession No.
4. TITLE AND SUBTITLE MOLECULAR ABSORPTION TEST AT 35 GHZ		5. Publication Date FEBRUARY 1982	
7. AUTHOR(S) Hans J. Liebe		6. Performing Organization Code NTIA/ITS3.4	
8. PERFORMING ORGANIZATION NAME AND ADDRESS National Telecommunications & Information Administration Institute for Telecommunication Sciences 3.4 325 Broadway Boulder, CO 80303		9. Project/Task/Work Unit No. 910 4428	
11. Sponsoring Organization Name and Address Defense Nuclear Agency (RAAE) Washington, DC 20305		10. Contract/Grant No.	
		12. Type of Report and Period Covered	
14. SUPPLEMENTARY NOTES		13.	
15. ABSTRACT (A 200-word or less factual summary of most significant information. If document includes a significant bibliography or literature survey, mention it here.) This report describes a laboratory experiment, which was conducted to find out if the absolute attenuation of a 35 GHz signal by the molecular species H₂O₂ (hydrogen peroxide), HNO₃ (nitric acid), NO₂ (nitrogen dioxide), and N₂O (nitrous oxide) exceeds a threshold value of 0.2 dB/km for concentrations reaching 500 ppm/vol in 1 atm of air. A resonance spectrometer was operated with a detection sensitivity of 0.1 dB/km to obtain pressure scans of attenuation and refraction for the pure gases at low pressures (< 1 kPa) and for binary mixtures at atmospheric pressures (> 50 kPa) using nitrogen as the inert, loss-free host gas. Model calculations of attenuation over the frequency range 10 to 50 GHz were performed for natural moist air and hot air (< 500 K) under sea level conditions. The measurements of the identified trace gas species produced little (i.e., > 0.2 dB/km) additional attenuation.			
16. Key Words (Alphabetical order, separated by semicolons) atmospheric 35 GHz attenuation; laboratory measurements; model calculations; sea level conditions; trace gas absorption			
17. AVAILABILITY STATEMENT <input checked="" type="checkbox"/> UNLIMITED. <input type="checkbox"/> FOR OFFICIAL DISTRIBUTION.		18. Security Class. (This report) UNCLASSIFIED	20. Number of pages 41
		19. Security Class. (This page) UNCLASSIFIED	21. Price:

